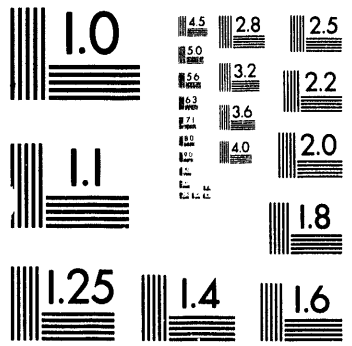
1.0
1.1
1.25
1.4
1.6
1.8
2.0
2.2
2.5
2.8
3.2
3.6
4.0
4.5
5.0
5.6
6.3
7.1
8.0
9.0
10.0
11.2
12.5
14.0
16.0
18.0
20.0
22.4
25.0
28.0
32.0
36.0
40.0
45.0
50.0
56.0
63.0
71.0
80.0
90.0
100.0
112.0
125.0
140.0
160.0
180.0
200.0
224.0
250.0
280.0
320.0
360.0
400.0
450.0
500.0
560.0
630.0
710.0
800.0
900.0
1000.0
1120.0
1250.0
1400.0
1600.0
1800.0
2000.0
2240.0
2500.0
2800.0
3200.0
3600.0
4000.0
4500.0
5000.0
5600.0
6300.0
7100.0
8000.0
9000.0
10000.0
11200.0
12500.0
14000.0
16000.0
18000.0
20000.0
22400.0
25000.0
28000.0
32000.0
36000.0
40000.0
45000.0
50000.0
56000.0
63000.0
71000.0
80000.0
90000.0
100000.0
112000.0
125000.0
140000.0
160000.0
180000.0
200000.0
224000.0
250000.0
280000.0
320000.0
360000.0
400000.0
450000.0
500000.0
560000.0
630000.0
710000.0
800000.0
900000.0
1000000.0
1120000.0
1250000.0
1400000.0
1600000.0
1800000.0
2000000.0
2240000.0
2500000.0
2800000.0
3200000.0
3600000.0
4000000.0
4500000.0
5000000.0
5600000.0
6300000.0
7100000.0
8000000.0
9000000.0
10000000.0
11200000.0
12500000.0
14000000.0
16000000.0
18000000.0
20000000.0
22400000.0
25000000.0
28000000.0
32000000.0
36000000.0
40000000.0
45000000.0
50000000.0
56000000.0
63000000.0
71000000.0
80000000.0
90000000.0
100000000.0
112000000.0
125000000.0
140000000.0
160000000.0
180000000.0
200000000.0
224000000.0
250000000.0
280000000.0
320000000.0
360000000.0
400000000.0
450000000.0
500000000.0
560000000.0
630000000.0
710000000.0
800000000.0
900000000.0
1000000000.0
1120000000.0
1250000000.0
1400000000.0
1600000000.0
1800000000.0
2000000000.0
2240000000.0
2500000000.0
2800000000.0
3200000000.0
3600000000.0
4000000000.0
4500000000.0
5000000000.0
5600000000.0
6300000000.0
7100000000.0
8000000000.0
9000000000.0
10000000000.0
11200000000.0
12500000000.0
14000000000.0
16000000000.0
18000000000.0
20000000000.0
22400000000.0
25000000000.0
28000000000.0
32000000000.0
36000000000.0
40000000000.0
45000000000.0
50000000000.0
56000000000.0
63000000000.0
71000000000.0
80000000000.0
90000000000.0
100000000000.0
112000000000.0
125000000000.0
140000000000.0
160000000000.0
180000000000.0
200000000000.0
224000000000.0
250000000000.0
280000000000.0
320000000000.0
360000000000.0
400000000000.0
450000000000.0
500000000000.0
560000000000.0
630000000000.0
710000000000.0
800000000000.0
900000000000.0
1000000000000.0
1120000000000.0
1250000000000.0
1400000000000.0
1600000000000.0
1800000000000.0
2000000000000.0
2240000000000.0
2500000000000.0
2800000000000.0
3200000000000.0
3600000000000.0
4000000000000.0
4500000000000.0
5000000000000.0
5600000000000.0
6300000000000.0
7100000000000.0
8000000000000.0
9000000000000.0
10000000000000.0
11200000000000.0
12500000000000.0
14000000000000.0
16000000000000.0
18000000000000.0
20000000000000.0
22400000000000.0
25000000000000.0
28000000000000.0
32000000000000.0
36000000000000.0
40000000000000.0
45000000000000.0
50000000000000.0
56000000000000.0
63000000000000.0
71000000000000.0
80000000000000.0
90000000000000.0
100000000000000.0
112000000000000.0
125000000000000.0
140000000000000.0
160000000000000.0
180000000000000.0
200000000000000.0
224000000000000.0
250000000000000.0
280000000000000.0
320000000000000.0
360000000000000.0
400000000000000.0
450000000000000.0
500000000000000.0
560000000000000.0
630000000000000.0
710000000000000.0
800000000000000.0
900000000000000.0
1000000000000000.0
1120000000000000.0
1250000000000000.0
1400000000000000.0
1600000000000000.0
1800000000000000.0
2000000000000000.0
2240000000000000.0
2500000000000000.0
2800000000000000.0
3200000000000000.0
3600000000000000.0
4000000000000000.0
4500000000000000.0
5000000000000000.0
5600000000000000.0
6300000000000000.0
7100000000000000.0
8000000000000000.0
9000000000000000.0
10000000000000000.0
11200000000000000.0
12500000000000000.0
14000000000000000.0
16000000000000000.0
18000000000000000.0
20000000000000000.0
22400000000000000.0
25000000000000000.0
28000000000000000.0
32000000000000000.0
36000000000000000.0
40000000000000000.0
45000000000000000.0
50000000000000000.0
56000000000000000.0
63000000000000000.0
71000000000000000.0
80000000000000000.0
90000000000000000.0
100000000000000000.0
112000000000000000.0
125000000000000000.0
140000000000000000.0
160000000000000000.0
180000000000000000.0
200000000000000000.0
224000000000000000.0
250000000000000000.0
280000000000000000.0
320000000000000000.0
360000000000000000.0
400000000000000000.0
450000000000000000.0
500000000000000000.0
560000000000000000.0
630000000000000000.0
710000000000000000.0
800000000000000000.0
900000000000000000.0
1000000000000000000.0
1120000000000000000.0
1250000000000000000.0
1400000000000000000.0
1600000000000000000.0
1800000000000000000.0
2000000000000000000.0
2240000000000000000.0
2500000000000000000.0
2800000000000000000.0
3200000000000000000.0
3600000000000000000.0
4000000000000000000.0
4500000000000000000.0
5000000000000000000.0
5600000000000000000.0
6300000000000000000.0
7100000000000000000.0
8000000000000000000.0
9000000000000000000.0
10000000000000000000.0
11200000000000000000.0
12500000000000000000.0
14000000000000000000.0
16000000000000000000.0
18000000000000000000.0
20000000000000000000.0
22400000000000000000.0
25000000000000000000.0
28000000000000000000.0
32000000000000000000.0
36000000000000000000.0
40000000000000000000.0
45000000000000000000.0
50000000000000000000.0
56000000000000000000.0
63000000000000000000.0
71000000000000000000.0
80000000000000000000.0
90000000000000000000.0
100000000000000000000.0
112000000000000000000.0
125000000000000000000.0
140000000000000000000.0
160000000000000000000.0
180000000000000000000.0
200000000000000000000.0
224000000000000000000.0
250000000000000000000.0
280000000000000000000.0
320000000000000000000.0
360000000000000000000.0
400000000000000000000.0
450000000000000000000.0
500000000000000000000.0
560000000000000000000.0
630000000000000000000.0
710000000000000000000.0
800000000000000000000.0
900000000000000000000.0
1000000000000000000000.0
1120000000000000000000.0
1250000000000000000000.0
1400000000000000000000.0
1600000000000000000000.0
1800000000000000000000.0
2000000000000000000000.0
2240000000000000000000.0
2500000000000000000000.0
2800000000000000000000.0
3200000000000000000000.0
3600000000000000000000.0
4000000000000000000000.0
4500000000000000000000.0
5000000000000000000000.0
5600000000000000000000.0
6300000000000000000000.0
7100000000000000000000.0
8000000000000000000000.0
9000000000000000000000.0
10000000000000000000000.0
11200000000000000000000.0
12500000000000000000000.0
14000000000000000000000.0
16000000000000000000000.0
18000000000000000000000.0
20000000000000000000000.0
22400000000000000000000.0
25000000000000000000000.0
28000000000000000000000.0
32000000000000000000000.0
36000000000000000000000.0
40000000000000000000000.0
45000000000000000000000.0
50000000000000000000000.0
56000000000000000000000.0
63000000000000000000000.0
71000000000000000000000.0
80000000000000000000000.0
90000000000000000000000.0
100000000000000000000000.0
112000000000000000000000.0
125000000000000000000000.0
140000000000000000000000.0
160000000000000000000000.0
180000000000000000000000.0
200000000000000000000000.0
224000000000000000000000.0
250000000000000000000000.0
280000000000000000000000.0
320000000000000000000000.0
360000000000000000000000.0
400000000000000000000000.0
450000000000000000000000.0
500000000000000000000000.0
560000000000000000000000.0
630000000000000000000000.0
710000000000000000000000.0
800000000000000000000000.0
900000000000000000000000.0
1000000000000000000000000.0
1120000000000000000000000.0
1250000000000000000000000.0
1400000000000000000000000.0
1600000000000000000000000.0
1800000000000000000000000.0
2000000000000000000000000.0
2240000000000000000000000.0
2500000000000000000000000.0
2800000000000000000000000.0
3200000000000000000000000.0
3600000000000000000000000.0
4000000000000000000000000.0
4500000000000000000000000.0
5000000000000000000000000.0
5600000000000000000000000.0
6300000000000000000000000.0
7100000000000000000000000.0
8000000000000000000000000.0
9000000000000000000000000.0
10000000000000000000000000.0
11200000000000000000000000.0
12500000000000000000000000.0
14000000000000000000000000.0
16000000000000000000000000.0
18000000000000000000000000.0
20000000000000000000000000.0
22400000000000000000000000.0
25000000000000000000000000.0
28000000000000000000000000.0
32000000000000000000000000.0
36000000000000000000000000.0
40000000000000000000000000.0
45000000000000000000000000.0
50000000000000000000000000.0
56000000000000000000000000.0
63000000000000000000000000.0
71000000000000000000000000.0
80000000000000000000000000.0
90000000000000000000000000.0
100000000000000000000000000.0
112000000000000000000000000.0
125000000000000000000000000.0
140000000000000000000000000.0
160000000000000000000000000.0
180000000000000000000000000.0
200000000000000000000000000.0
224000000000000000000000000.0
250000000000000000000000000.0
280000000000000000000000000.0
320000000000000000000000000.0
360000000000000000000000000.0
400000000000000000000000000.0
450000000000000000000000000.0
500000000000000000000000000.0
560000000000000000000000000.0
630000000000000000000000000.0
710000000000000000000000000.0
800000000000000000000000000.0
900000000000000000000000000.0
1000000000000000000000000000.0
1120000000000000000000000000.0
1250000000000000000000000000.0
1400000000000000000000000000.0
1600000000000000000000000000.0
1800000000000000000000000000.0
2000000000000000000000000000.0
2240000000000000000000000000.0
2500000000000000000000000000.0
2800000000000000000000000000.0
3200000000000000000000000000.0
3600000000000000000000000000.0
4000000000000000000000000000.0
4500000000000000000000000000.0
5000000000000000000000000000.0
5600000000000000000000000000.0
6300000000000000000000000000.0
7100000000000000000000000000.0
8000000000000000000000000000.0
9000000000000000000000000000.0
10000000000000000000000000000.0
11200000000000000000000000000.0
12500000000000000000000000000.0
14000000000000000000000000000.0
16000000000000000000000000000.0
18000000000000000000000000000.0
20000000000000000000000000000.0
22400000000000000000000000000.0
25000000000000000000000000000.0
28000000000000000000000000000.0
32000000000000000000000000000.0
36000000000000000000000000000.0
40000000000000000000000000000.0
45000000000000000000000000000.0
50000000000000000000000000000.0
56000000000000000000000000000.0
63000000000000000000000000000.0
71000000000000000000000000000.0
80000000000000000000000000000.0
90000000000000000000000000000.0
100000000000000000000000000000.0
112000000000000000000000000000.0
125000000000000000000000000000.0
140000000000000000000000000000.0
160000000000000000000000000000.0
180000000000000000000000000000.0
200000000000000000000000000000.0
224000000000000000000000000000.0
250000000000000000000000000000.0
280000000000000000000000000000.0
320000000000000000000000000000.0
360000000000000000000000000000.0
400000000000000000000000000000.0
450000000000000000000000000000.0
500000000000000000000000000000.0
560000000000000000000000000000.0
630000000000000000000000000000.0
710000000000000000000000000000.0
800000000000000000000000000000.0
900000000000000000000000000000.0
1000000000000000000000000000000.0
1120000000000000000000000000000.0
1250000000000000000000000000000.0
1400000000000000000000000000000.0
1600000000000000000000000000000.0
1800000000000000000000000000000.0
2000000000000000000000000000000.0
2240000000000000000000000000000.0
2500000000000000000000000000000.0
2800000000000000000000000000000.0
3200000000000000000000000000000.0
3600000000000000000000000000000.0
4000000000000000000000000000000.0
4500000000000000000000000000000.0
5000000000000000000000000000000.0
5600000000000000000000000000000.0
6300000000000000000000000000000.0
7100000000000000000000000000000.0
8000000000000000000000000000000.0
9000000000000000000000000000000.0
10000000000000000000000000000000.0
11200000000000000000000000000000.0
12500000000000000000000000000000.0
14000000000000000000000000000000.0
16000000000000000000000000000000.0
18000000000000000000000000000000.0
20000000000000000000000000000000.0
22400000000000000000000000000000.0
25000000000000000000000000000000.0
28000000000000000000000000000000.0
32000000000000000000000000000000.0
36000000000000000000000000000000.0
40000000000000000000000000000000.0
45000000000000000000000000000000.0
50000000000000000000000000000000.0
56000000000000000000000000000000.0
63000000000000000000000000000000.0
71000000000000000000000000000000.0
80000000000000000000000000000000.0
90000000000000000000000000000000.0
100000000000000000000000000000000.0
112000000000000000000000000000000.0
125000000000000000000000000000000.0
140000000000000000000000000000000.0
160000000000000000000000000000000.0
180000000000000000000000000000000.0
200000000000000000000000000000000.0
224000000000000000000000000000000.0
250000000000000000000000000000000.0
280000000000000000000000000000000.0
320000000000000000000000000000000.0
360000000000000000000000000000000.0
400000000000000000000000000000000.0
450000000000000000000000000000000.0
500000000000000000000000000000000.0
560000000000000000000000000000000.0
630000000000000000000000000000000.0
710000000000000000000000000000000.0
800000000000000000000000000000000.0
900000000000000000000000000000000.0
1000000000000000000000000000000000.0
1120000000000000000000000000000000.0
1250000000000000000000000000000000.0
1400000000000000000000000000000000.0
1600000000000000000000000000000000.0
1800000000000000000000000000000000.0
2000000000000000000000000000000000.0
2240000000000000000000000000000000.0
2500000000000000000000000000000000.0
2800000000000000000000000000000000.0
3200000000000000000000000000000000.0
3600000000000000000000000000000000.0
4000000000000000000000000000000000.0
4500000000000000000000000000000000.0
5000000000000000000000000000000000.0
5600000000000000000000000000000000.0
6300000000000000000000000000000000.0
7100000000000000000000000000000000.0
8000000000000000000000000000000000.0
9000000000000000000000000000000000.0
10000000000000000000000000000000000.0
11200000000000000000000000000000000.0
12500000000000000000000000000000000.0
14000000000000000000000000000000000.0
16000000000000000000000000000000000.0
18000000000000000000000000000000000.0
20000000000000000000000000000000000.0
22400000000000000000000000000000000.0
25000000000000000000000000000000000.0
28000000000000000000000000000000000.0
32000000000000000000000000000000000.0
36000000000000000000000000000000000.0
40000000000000000000000000000000000.0
45000000000000000000000000000000000.0
50000000000000000000000000000000000.0
56000000000000000000000000000000000.0
63000000000000000000000000000000000.0
71000000000000000000000000000000000.0
80000000000000000000000000000000000.0
90000000000000000000000000000000000.0
100000000000000000000000000000000000.0
112000000000000000000000000000000000.0
125000000000000000000000000000000000.0
140000000000000000000000000000000000.0
160000000000000000000000000000000000.0
180000000000000000000000000000000000.0
200000000000000000000000000000000000.0
224000000000000000000000000000000000.0
250000000000000000000000000000000000.0
280000000000000000000000000000000000.0
320000000000000000000000000000000000.0
360000000000000000000000000000000000.0
400000000000000000000000000000000000.0
450000000000000000000000000000000000.0
500000000000000000000000000000000000.0
560000000000000000000000000000000000.0
630000000000000000000000000000000000.0
710000000000000000000000000000000000.0
800000000000000000000000000000000000.0
900000000000000000000000000000000000.0
1000000000000000000000000000000000000.0
1120000000000000000000000000000000000.0
1250000000000000000000000000000000000.0
1400000000000000000000000000000000000.0
1600000000000000000000000000000000000.0
1800000000000000000000000000000000000.0
2000000000000000000000000000000000000.0
2240000000000000000000000000000000000.0
2500000000000000000000000000000000000.0
2800000000000000000000000000000000000.0
3200000000000000000000000000000000000.0
3600000000000000000000000000000000000.0
4000000000000000000000000000000000000.0
4500000000000000000000000000000000000.0
5000000000000000000000000000000000000.0
5600000000000000000000000000000000000.0
6300000000000000000000000000000000000.0
7100000000000000000000000000000000000.0
8000000000000000000000000000000000000.0
9000000000000000000000000000000000000.0
10000000000000000000000000000000000000.0
11200000000000000000000000000000000000.0
12500000000000000000000000000000000000.0
14000000000000000000000000000000000000.0
16000000000000000000000000000000000000.0
18000000000000000000000000000000000000.0
20000000000000000000000000000000000000.0
22400000000000000000000000000000000000.0
25000000000000000000000000000000000000.0
28000000000000000000000000000000000000.0
32000000000000000000000000000000000000.0
36000000000000000000000000000000000000.0
40000000000000000000000000000000000000.0
45000000000000000000000000000000000000.0
50000000000000000000000000000000000000.0
56000000000000000000000000000000000000.0
63000000000000000000000000000000000000.0
71000000000000000000000000000000000000.0
80000000000000000000000000000000000000.0
90000000000000000000000000000000000000.0
100000000000000000000000000000000000000.0
112000000000000000000000000000000000000.0
125000000000000000000000000000000000000.0
140000000000000000000000000000000000000.0
160000000000000000000000000000000000000.0
180000000000000000000000000000000000000.0
200000000000000000000000000000000000000.0
224000000000000000000000000000000000000.0
250000000000000000000000000000000000000.0
280000000000000000000000000000000000000.0
320000000000000000000000000000000000000.0
360000000000000000000000000000000000000.0
400000000000000000000000000000000000000.0
450000000000000000000000000000000000000.0
500000000000000000000000000000000000000.0
560000000000000000000000000000000000000.0
630000000000000000000000000000000000000.0
710000000000000000000000000000000000000.0
800000000000000000000000000000000000000.0
900000000000000000000000000000000000000.0
1000000000000000000000000000000000000000.0
1120000000000000000000000000000000000000.0
1250000000000000000000000000000000000000.0
1400000000000000000000000000000000000000.0
1600000000000000000000000000000000000000.0
1800000000000000000000000000000000000000.0
2000000000000000000000000000000000000000.0
2240000000000000000000000000000000000000.0
2500000000000000000000000000000000000000.0
2800000000000000000000000000000000000000.0
3200000000000000000000000000000000000000.0
3600000000000000000000000000000000000000.0
4000000000000000000000000000000000000000.0
4500000000000000000000000000000000000000.0
5000000000000000000000000000000000000000.0
5600000000000000000000000000000000000000.0
6300000000000000000000000000000000000000.0
7100000000000000000000000000000000000000.0
8000000000000000000000000000000000000000.0
9000000000000000000000000000000000000000.0
10000000000000000000000000000000000000000.0
11200000000000000000000000000000000000000.0
12500000000000000000000000000000000000000.0
14000000000000000000000000000000000000000.0
16000000000000000000000000000000000000000.0
18000000000000000000000000000000000000000.0
20000000000000000000000000000000000000000.0
22400000000000000000000000000000000000000.0
25000000000000000000000000000000000000000.0
28000000000000000000000000000000000000000.0
32000000000000000000000000000000000000000.0
36000000000000000000000000000000000000000.0
40000000000000000000000000000000000000000.0
45000000000000000000000000000000000000000.0
50000000000000000000000000000000000000000.0
56000000000000000000000000000000000000000.0
63000000000000000000000000000000000000000.0
71000000000000000000000000000000000000000.0
80000000000000000000000000000000000000000.0
90000000000000000000000000000000000000000.0
100000000000000000000000000000000000000000.0
112000000000000000000000000000000000000000.0
125000000000000000000000000000000000000000.0
140000000000000000000000000000000000000000.0
160000000000000000000000000000000000000000.0
180000000000000000000000000000000000000000.0
200000000000000000000000000000000000000000.0
224000000000000000000000000000000000000000.0
250000000000000000000000000000000000000000.0
280000000000000000000000000000000000000000.0
320000000000000000000000000000000000000000.0
360000000000000000000000000000000000000000.0
400000000000000000000000000000000000000000.0
450000000000000000000000000000000000000000.0
500000000000000000000000000000000000000000.0
560000000000000000000000000000000000000000.0
630000000000000000000000000000000000000000.0
710000000000000000000000000000000000000000.0
800000000000000000000000000000000000000000.0
900000000000000000000000000000000000000000.0
1000000000000000000000000000000000000000000.0
1120000000000000000000000000000000000000000.0
1250000000000000000000000000000000000000000.0
1400000000000000000000000000000000000000000.0
1600000000000000000000000000000000000000000.0
1800000000000000000000000000000000000000000.0
2000000000000000000000000000000000000000000.0
2240000000000000000000000000000000000000000.0
2500000000000000000000000000000000000000000.0
2800000000000000000000000000000000000000000.0
3200000000000000000000000000000000000000000.0
3600000000000000000000000000000000000000000.0
4000000000000000000000000000000000000000000.0
4500000000000000000000000000000000000000000.0
5000000000000000000000000000000000000000000.0
5600000000000000000000000000000000000000000.0
6300000000000000000000000000000000000000000.0
7100000000000000000000000000000000000000000.0
8000000000000000000000000000000000000000000.0
9000000000000000000000000000000000000000000.0
10000000000000000000000000000000000000000000.0
11200000000000000000000000000000000000000000.0
12500000000000000000000000000000000000000000.0
14000000000000000000000000000000000000000000.0
16000000000000000000000000000000000000000000.0
18000000000000000000000000000000000000000000.0
20000000000000000000000000000000000000000000.0
22400000000000000000000000000000000000000000.0
25000000000000000000000000000000000000000000.0
28000000000000000000000000000000000000000000.0
32000000000000000000000000000000000000000000.0
36000000000000000000000000000000000000000000.0
40000000000000000000000000000000000000000000.0
45000000000000000000000000000000000000000000.0
50000000000000000000000000000000000000000000.0
56000000000000000000000000000000000000000000.0
63000000000000000000000000000000000000000000.0
71000000000000000000000000000000000000000000.0
80000000000000000000000000000000000000000000.0
90000000000000000000000000000000000000000000.0
100000000000000000000000000000000000000000000.0
112000000000000000000000000000000000000000000.0
125000000000000000000000000000000000000000000.0
140000000000000000000000000000000000000000000.0
160000000000000000000000000000000000000000000.0
180000000000000000000000000000000000000000000.0
200000000000000000000000000000000000000000000.0
224000000000000000000000000000000000000000000.0
250000000000000000000000000000000000000000000.0
280000000000000000000000000000000000000000000.0
320000000000000000000000000000000000000000000.0
360000000000000000000000000000000000000000000.0
400000000000000000000000000000000000000000000.0
450000000000000000000000000000000000000000000.0
500000000000000000000000000000000000000000000.0
560000000000000000000000000000000000000000000.0
630000000000000000000000000000000000000000000.0
710000000000000000000000000000000000000000000.0
800000000000000000000000000000000000000000000.0
900000000000000000000000000000000000000000000.0
1000000000000000000000000000000000000000000000.0
1120000000000000000000000000000000000000000000.0
1250000000000000000000000000000000000000000000.0
1400000000000000000000000000000000000000000000.0
1600000000000000000000000000000000000000000000.0
1800000000000000000000000000000000000000000000.0
2000000000000000000000000000000000000000000000.0
2240000000000000000000000000000000000000000000.0
2500000000000000000000000000000000000000000000.0
2800000000000000000000000000000000000000000000.0
3200000000000000000000000000000000000000000000.0
3600000000000000000000000000000000000000000000.0
4000000000000000000000000000000000000000000000.0
4500000000000000000000000000000000000000000000.0
5000000000000000000000000000000000000000000000.0
5600000000000000000000000000000000000000000000.0
6300000000000000000000000000000000000000000000.0
7100000000000000000000000000000000000000000000.0
8000000000000000000000000000000000000000000000.0
9000000000000000000000000000000000000000000000.0
10000000000000000000000000000000000000000000000.0
11200000000000000000000000000000000000000000000.0
12500000000000000000000000000000000000000000000.0
14000000000000000000000000000000000000000000000.0
16000000000000000000000000000000000000000000000.0
18000000000000000000000000000000000000000000000.0
20000000000000000000000000000000000000000000000.0
22400000000000000000000000000000000000000000000.0
25000000000000000000000000000000000000000000000.0
28000000000000000000000000000000000000000000000.0
32000000000000000000000000000000000000000000000.0
36000000000000000000000000000000000000000000000.0
40000000000000000000000000000000000000000000000.0
45000000000000000000000000000000000000000000000.0
50000000000000000000000000000000000000000000000.0
56000000000000000000000000000000000000000000000.0
63000000000000000000000000000000000000000000000.0
71000000000000000000000000000000000000000000000.0
80000000000000000000000000000000000000000000000.0
90000000000000000000000000000000000000000000000.0
100000000000000000000000000000000000000000000000.0
112000000000000000000000000000000000000000000000.0
125000000000000000000000000000000000000000000000.0
140000000000000000000000000000000000000000000000.0
160000000000000000000000000000000000000000000000.0
180000000000000000000000000000000000000000000000.0
200000000000000000000000000000000000000000000000.0
224000000000000000000000000000000000000000000000.0
250000000000000000000000000000000000000000000000.0
280000000000000000000000000000000000000000000000.0
320000000000000000000000000000000000000000000000.0
360000000000000000000000000000000000000000000000.0
400000000000000000000000000000000000000000000000.0
450000000000000000000000000000000000000000000000.0
500000000000000000000000000000000000000000000000.0
560000000000000000000000000000000000000000000000.0
630000000000000000000000000000000000000000000000.0
710000000000000000000000000000000000000000000000.0
800000000000000000000000000000000000000000000000.0
900000000000000000000000000000000000000000000000.0
1000000000000000000000000000000000000000000000000.0
1120000000000000000000000000000000000000000000000.0
1250000000000000000000000000000000000000000000000.0
1400000000000000000000000000000000000000000000000.0
1600000000000000000000000000000000000000000000000.0
1800000000000000000000000000000000000000000000000.0
2000000000000000000000000000000000000000000000000.0
2240000000000000000000000000000000000000000000000.0
2500000000000000000000000000000000000000000000000.0
2800000000000000000000000000000000000000000000000.0
3200000000000000000000000000000000000000000000000.0
3600000000000000000000000000000000000000000000000.0
4000000000000000000000000000000000000000000000000.0
4500000000000000000000000000000000000000000000000.0
5000000000000000000000000000000000000000000000000.0
5600000000000000000000000000000000000000000000000.0
6300000000000000000000000000000000000000000000000.0
7100000000000000000000000000000000000000000000000.0
8000000000000000000000000000000000000000000000000.0
9000000000000000000000000000000000000000000000000.0
10000000000000000000000000000000000000000000000000.0
11200000000000000000000000000000000000000000000000.0
12500000000000000000000000000000000000000000000000.0
14000000000000000000000000000000000000000000000000.0
16000000000000000000000000000000000000000000000000.0
18000000000000000000000000000000000000000000000000.0
20000000000000000000000000000000000000000000000000.0
22400000000000000000000000000000000000000000000000.0
25000000000000000000000000000000000000000000000000.0
28000000000000000000000000000000000000000000000000.0
32000000000000000000000000000000000000000000000000.0
36000000000000000000000000000000000000000000000000.0
40000000000000000000000000000000000000000000000000.0
45000000000000000000000000000000000000000000000000.0
50000000000000000000000000000000000000000000000000.0
56000000000000000000000000000000000000000000000000.0
63000000000000000000000000000000000000000000000000.0
71000000000000000000000000000000000000000000000000.0
80000000000000000000000000000000000000000000000000.0
90000000000000000000000000000000000000000000000000.0
100000000000000000000000000000000000000000000000000.0
112000000000000000000000000000000000000000000000000.0
125000000000000000000000000000000000000000000000000.0
140000000000000000000000000000000000000000000000000.0
160000000000000000000000000000000000000000000000000.0
180000000000000000000000000000000000000000000000000.0
200000000000000000000000000000000000000000000000000.0
224000000000000000000000000000000000000000000000000.0
250000000000000000000000000000000000000000000000000.0
280000000000000000000000000000000000000000000000000.0
320000000000000000000000000000000000000000000000000.0
360000000000000000000000000000000000000000000000000.0
400000000000000000000000000000000000000000000000000.0
450000000000000000000000000000000000000000000000000.0
500000000000000000000000000000000000000000000000000.0
560000000000000000000000000000000000000000000000000.0
630000000000000000000000000000000000000000000000000.0
710000000000000000000000000000000000000000000000000.0
800000000000000000000000000000000000000000000000000.0
900000000000000000000000000000000000000000000000000.0
1000000000000000000000000000000000000000000000000000.0
1120000000000000000000000000000000000000000000000000.0
1250000000000000000000000000000000000000000000000000.0
1400000000000000000000000000000000000000000000000000.0
1600000000000000000000000000000000000000000000000000.0
1800000000000000000000000000000000000000000000000000.0
2000000000000000000000000000000000000000000000000000.0
2240000000000000000000000000000000000000000000000000.0
2500000000000000000000000000000000000000000000000000.0
2800000000000000000000000000000000000000000000000000.0
3200000000000000000000000000000000000000000000000000.0
3600000000000000000000000000000000000000000000000000.0
4000000000000000000000000000000000000000000000000000.0
4500000000000000000000000000000000000000000000000000.0
5000000000000000000000000000000000000000000000000000.0
5600000000000000000000000000000000000000000000000000.0
6300000000000000000000000000000000000000000000000000.0
7100000000000000000000000000000000000000000000000000.0
8000000000000000000000000000000000000000000000000000.0
9000000000000000000000000000000000000000000000000000.0
10000000000000000000000000000000000000000000000000000.0
11200000000000000000000000000000000000000000000000000.0
12500000000000000000000000000000000000000000000000000.0
14000000000000000000000000000000000000000000000000000.0
16000000000000000000000000000000000000000000000000000.0
18000000000000000000000000000000000000000000000000000.0
20000000000000000000000000000000000000000000000000000.0
22400000000000000000000000000000000000000000000000000.0
25000000000000000000000000000000000000000000000000000.0
28000000000000000000000000000000000000000000000000000.0
32000000000000000000000000000000000000000000000000000.0
36000000000000000000000000000000000000000000000000000.0
40000000000000000000000000000000000000000000000000000.0
45000000000000000000000000000000000000000000000000000.0
50000000000000000000000000000000000000000000000000000.0
56000000000000000000000000000000000000000000000000000.0
63000000000000000000000000000000000000000000000000000.0
71000000000000000000000000000000000000000000000000000.0
80000000000000000000000000000000000000000000000000000.0
90000000000000000000000000000000000000000000000000000.0
100000000000000000000000000000000000000000000000000000.0
112000000000000000000000000000000000000000000000000000.0
125000000000000000000000000000000000000000000000000000.0
140000000000000000000000000000000000000000000000000000.0
160000000000000000000000000000000000000000000000000000.0
180000000000000000000000000000000000000000000000000000.0
200000000000000000000000000000000000000000000000000000.0
224000000000000000000000000000000000000000000000000000.0
250000000000000000000000000000000000000000000000000000.0
280000000000000000000000000000000000000000000000000000.0
320000000000000000000000000000000000000000000000000000.0
360000000000000000000000000000000000000000000000000000.0
400000000000000000000000000000000000000000000000000000.0
450000000000000000000000000000000000000000000000000000.0
500000000000000000000000000000000000000000000000000000.0
560000000000000000000000000000000000000000000000000000.0
630000000000000000000000000000000000000000000000000000.0
710000000000000000000000000000000000000000000000000000.0
800000000000000000000000000000000000000000000000000000.0
900000000000000000000000000000000000000000000000000000.0
1000000000000000000000000000000000000000000000000000000.0
1120000000000000000000000000000000000000000000000000000.0
1250000000000000000000000000000000000000000000000000000.0
1400000000000000000000000000000000000000000000000000000.0
1600000000000000000000000000000000000000000000000000000.0
1800000000000000000000000000000000000000000000000000000.0
2000000000000000000000000000000000000000000000000000000.0
2240000000000000000000000000000000000000000000000000000.0
2500000000000000000000000000000000000000000000000000000.0
2800000000000000000000000000000000000000000000000000000.0
3200000000000000000000000000000000000000000000000000000.0
3600000000000000000000000000000000000000000000000000000.0
4000000000000000000000000000000000000000000000000000000.0
4500000000000000000000000000000000000000000000000000000.0
5000000000000000000000000000000000000000000000000000000.0
5600000000000000000000000000000000000000000000000000000.0
6300000000000000000000000000000000000000000000000000000.0
7100000000000000000000000000000000000000000000000000000.0
8000000000000000000000000000000000000000000000000000000.0
9000000000000000000000000000000000000000000000000000000.0
10000000000000000000000000000000000000000000000000000000.0
11200000000000000000000000000000000000000000000000000000.0
12500000000000000000000000000000000000000000000000000000.0
14000000000000000000000000000000000000000000000000000000.0
16000000000000000000000000000000000000000000000000000000.0
18000000000000000000000000000000000000000000000000000000.0
20000000000000000000000000000000000000000000000000000000.0
22400000000000000000000000000000000000000000000000000000.0
25000000000000000000000000000000000000000000000000000000.0
28000000000000000000000000000000000000000000000000000000.0
32000000000000000000000000000000000000000000000000000000.0
36000000000000000000000000000000000000000000000000000000.0
40000000000000000000000000000000000000000000000000000000.0
45000000000000000000000000000000000000000000000000000000.0
50000000000000000000000000000000000000000000000000000000.0
56000000000000000000000000000000000000000000000000000000.0
63000000000000000000000000000000000000000000000000000000.0
71000000000000000000000000000000000000000000000000000000.0
80000000000000000000000000000000000000000000000000000000.0
90000000000000000000000000000000000000000000000000000000.0
100000000000000000000000000000000000000000000000000000000.0
112000000000000000000000000000000000000000000000000000000.0
125000000000000000000000000000000000000000000000000000000.0
140000000000000000000000000000000000000000000000000000000.0
160000000000000000000000000000000000000000000000000000000.0
180000000000000000000000000000000000000000000000000000000.0
200000000000000000000000000000000000000000000000000000000.0
224000000000000000000000000000000000000000000000000000000.0
250000000000000000000000000000000000000000000000000000000.0
280000000000000000000000000000000000000000000000000000000.0
320000000000000000000000000000000000000000000000000000000.0
360000000000000000000000000000000000000000000000000000000.0
400000000000000000000000000000000000000000000000000000000.0
450000000000000000000000000000000000000000000000000000000.0
500000000000000000000000000000000000000000000000000000000.0
560000000000000000000000000000000000000000000000000000000.0
630000000000000000000000000000000000000000000000000000000.0
710000000000000000000000000000000000000000000000000000000.0
800000000000000000000000000000000000000000000000000000000.0
900000000000000000000000000000000000000000000000000000000.0
1000000000000000000000000000000000000000000000000000000000.0
1120000000000000000000000000000000000000000000000000000000.0
1250000000000000000000000000000000000000000000000000000000.0
1400000000000000000000000000000000000000000000000000000000.0
1600000000000000000000000000000000000000000000000000000000.0
1800000000000000000000000000000000000000000000000000000000.0
2000000000000000000000000000000000000000000000000000000000.0
2240000000000000000000000000000000000000000000000000000000.0
2500000000000000000000000000000000000000000000000000000000.0
2800000000000000000000000000000000000000000000000000000000.0
3200000000000000000000000000000000000000000000000000000000.0
3600000000000000000000000000000000000000000000000000000000.0
4000000000000000000000000000000000000000000000000000000000.0
4500000000000000000000000000000000000000000000000000000000.0
5000000000000000000000000000000000000000000000000000000000.0
5600000000000000000000000000000000000000000000000000000000.0
6300000000000000000000000000000000000000000000000000000000.0
7100000000000000000000000000000000000000000000000000000000.0
8000000000000000000000000000000000000000000000000000000000.0
9000000000000000000000000000000000000000000000000000000000.0
10000000000000000000000000000000000000000000000000000000000.0
11200000000000000000000000000000000000000000000000000000000.0
12500000000000000000000000000000000000000000000000000000000.0
14000000000000000000000000000000000000000000000000000000000.0
16000000000000000000000000000000000000000000000000000000000.0
18000000000000000000000000000000000000000000000000000000000.0
20000000000000000000000000000000000000000000000000000000000.0
22400000000000000000000000000000000000000000000000000000000.0
25000000000000000000000000000000000000000000000000000000000.0
28000000000000000000000000000000000000000000000000000000000.0
32000000000000000000000000000000000000000000000000000000000.0
36000000000000000000000000000000000000000000000000000000000.0
40000000000000000000000000000000000000000000000000000000000.0
45000000000000000000000000000000000000000000000000000000000.0
50000000000000000000000000000000000000000000000000000000000.0
56000000000000000000000000000000000000000000000000000000000.0
63000000000000000000000000000000000000000000000000000000000.0
71000000000000000000000000000000000000000000000000000000000.0
80000000000000000000000000000000000000000000000000000000000.0
90000000000000000000000000000000000000000000000000000000000.0
100000000000000000000000000000000000000000000000000000000000.0
112000000000000000000000000000000000000000000000000000000000.0
125000000000000000000000000000000000000000000000000000000000.0
140000000000000000000000000000000000000000000000000000000000.0
160000000000000000000000000000000000000000000000000000000000.0
180000000000000000000000000000000000000000000000000000000000.0
200000000000000000000000000000000000000000000000000000000000.0
224000000000000000000000000000000000000000000000000000000000.0
250000000000000000000000000000000000000000000000000000000000.

1 of 1

IS-T 1669

Characterization of ZnS-GaP Nano-composites

by

Voiles, Todd

MS Thesis submitted to Iowa State University

Ames Laboratory, U.S. DOE
Iowa State University
Ames, Iowa 50011

Date Transmitted: December 9, 1993

PREPARED FOR THE U.S. DEPARTMENT OF ENERGY
UNDER CONTRACT NO. W-7405-Eng-82.

DISCLAIMER

DEDICATION

This work is dedicated to both my parents and my loving future wife, without whose encouragement and love I would not have been able to complete my studies.

TABLE OF CONTENTS

LIST OF FIGURES

LIST OF TABLES

INTRODUCTION

The search for an infra-red (IR) window material with both good mechanical and IR properties has been in progress for more than 30 years. The IR range of greatest interest, 8-12 μm, is the typical radiation wavelength range for room temperature objects. Future infra-red windows are expected to be used on super-sonic aircraft and missiles and must, therefore perform in hostile environments (i.e. survive impacts with raindrops and dust particles at high speed). These windows must exhibit good IR transmittance, high melting temperatures, good rain erosion resistance, and excellent thermal shock resistance.[1] Table 1 shows some relevant physical properties of a number of IR window material candidates. Examination of this table indicates that, based on the physical properties, the material of choice should be diamond. Diamond's drawback is the great difficulty of processing useful quantities into usable window shapes. While diamond may be the ultimate solution for an IR transmitting material for severe environments, the present need can be met by a material that has adequate properties and is relatively easy to process.[1]

Among the other compounds shown in Table 1, ZnS (Figure 1) appears to meet most of the requirements, lacking only in mechanical properties, especially hardness.[1] ZnS exists in two distinct crystal structures, cubic (sphalerite) and hexagonal (wurtzite), with the cubic dominant at low temperatures (Figure 1 and Table 2). Two methods can be combined to improve the lacking qualities of ZnS, use of nanocrystalline ZnS powders and impregnating these powders with GaP (Figure 1), thus forming a nano-scale composite.

Dunn found that doping ZnS with gallium increased its hardness by 80%.[2] GaP is a logical "vehicle material" for the introduction of gallium into ZnS because of the following reasons. GaP has a higher resistance to rain erosion than ZnS and

Table 1. Physical properties of infra-red transparent materials

Material	Melting Point °C	Transmittance Range μm	Refractive Index at 4.0 μm	Knoop Hardness kg/mm²	Young's Modulus GPa	Rupture Modulus MPa	Thermal Expansion $10^{-6}C^{-1}$	Thermal Conductivity w/cmK	Density g/cm³
KCl	776	0.4-18.0	1.50	10	27	6	20.3		1.98
KBr	734	0.4-21.0	1.50		25	5	40.3		2.75
AgCl	445	0.5-20.0	2.00	10	23		35.7		5.56
MgF_2	1266	0.2-6.0	1.34	580	114	>150	10.4		
CaF_2	1360	0.2-8.0	1.38	160	77	37	19.2		3.18
ZnS	1830	1.0-10.0	2.20	250	75	105	7.4	0.17	4.08
ZnSe	>1100	0.6-15.0	2.37	110	66	55	7.4		
GaAs	1238	1.3-12.2	3.70	750	93	72	7.0	0.53	5.32
GaP	1467			845	102		5.3	0.97	4.13
Si	1410	1.4-6.0	3.35	1160	192	170	3.0	1.41	2.33
Ge	937	2.-12.3	4.0	850	103	93	7.0	0.60	5.32
C(Diamond)	--			9000	1050		1.0	26.0	3.52
SiO_2	>1600	0.2-3.5	1.5-2.0	460	75	69	0.5		>2.20
Al_2O_3	2020	0.2-5.0	1.70	>1050	>217	>175	7.4		3.96
$MgAl_2O_4$	>1500	0.3-5.0	1.72	1300	266	>175	7.3		3.6
$CaLa_2S_4$	1810	2.0-20	(2.0)	570	96		14.8		
Sulfide Glass	500-600	0.8-8.2	2.37	110		16	26.0		>3.8
Selenide Glass	>500	1.0-12.0	2.50	170	23	15	12.5		

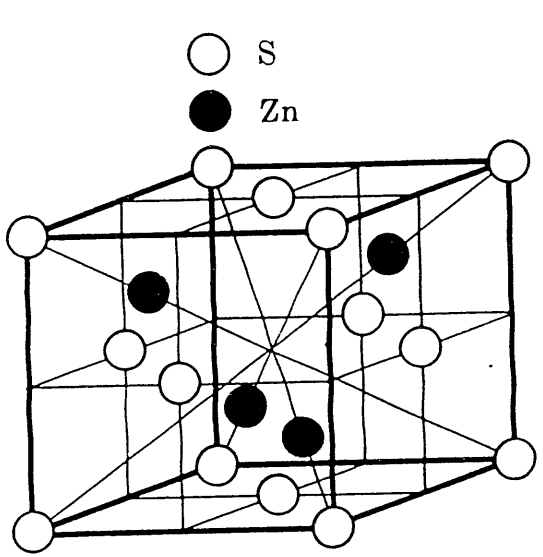

Zinc blende

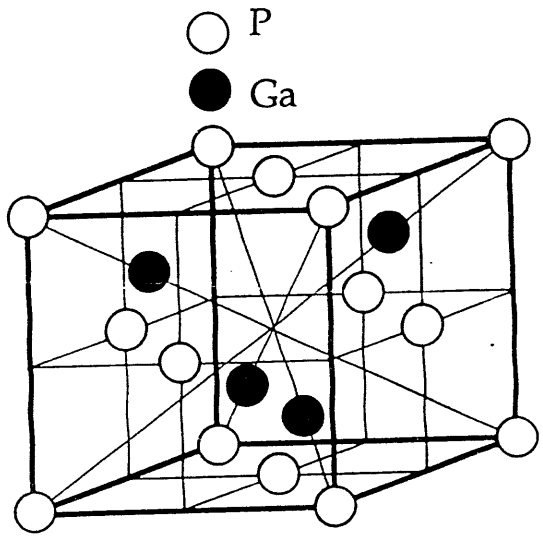

Zinc blende

	Crystal Structure (Low Temp)	Lattice Parameters	Crystal Sturcture (High Temp)	Lattice Paramaters
ZnS	Zinc Blende	a = b = c = 0.54109 nm	Hexagonal	a = b = 0.382 nm c = 0.626 nm
GaP	Zinc Blende	a = b = c = 0.54505 nm	Hexagonal	a = b = 0.376 nm c = 1.57 nm

Figure 1. Crystal structure of ZnS and GaP

Table 2. Commonly seen XRD peaks for ZnS from theoretical lattice parameters

Cubic ZnS			Hexagonal ZnS		
Peak (hkl)	d-spacing(Å)	2-θ	Peak (hkl	d-spacing(Å)	2-θ
111	3.123	28.57	100	3.310	26.93
002	2.705	33.11	002	3.131	28.51
112	2.209	40.85	011	2.926	30.54
022	1.913	47.53	012	2.275	39.62
013	1.711	53.56	013	1.765	51.78
113	1.631	56.40	200	1.655	55.52
222	1.562	59.15	112	1.631	56.40
			201	1.600	57.60

Table 3. Average grain sizes for ZnS samples by both XRD and TEM methods

Sample	Heat treatment	Avg. grain size by XRD[10]	Avg. grain size by TEM
ZnS #18	as-prepared	8 nm	14 nm
ZnS #18	500°C for 24 hours	24 nm	42 nm
ZnS #18	600°C for 20 hours	41 nm	66 nm

its lattice parameters differ by only 1.8% with ZnS (Figure 1).[3] Both ZnS and GaP are semiconductors; ZnS having a direct band gap of 3.58 eV while GaP has an indirect band gap of 2.24 eV[3]; their thermal expansion coefficients differ by less than 25%.

Nano-crystalline materials may be described as solids that consist of small crystalline grains separated from each other by a grain boundary.[4] Although the exact reason is not known, the unique atomic arrangement present when the microstructure of a material is reduced to the nano-scale level results in new and different properties being exhibited. Reduction of the coefficient of thermal expansion has been seen[5] as well as melting point depression[6] and an increase in hardness[7].

By definition, nano-crystalline materials are polycrystalline and for polycrystalline bodies to be used in an IR window a uniform final microstructure is needed. In addition optical materials must be sintered to full density as even minimal residual porosity causes detrimental scattering.[8] The microstructure formed during densification of bodies is largely determined by the characteristics of the starting powder and by the green compact's microstructure. Although starting powders consisting of spherical, submicron particles are normally considered desirable, there is no general agreement as to whether particle assemblies with a narrow or wide size distribution are more preferable for achieving a theoretically dense uniform microstructure. It is well-known that random packing of particles with a large size distribution yields denser green compacts than do mono-sized particles.[9] On the other hand, mono-size powder assemblies are believed to sinter more uniformly.[9]

A combination of the proposed enhancement techniques described above would ideally lead to a composite material of superior strength and mechanical properties for use in an advanced IR window. Such a composite material could be formed if nanocrystalline ZnS powders could be synthesized and impregnated with a Ga containing compound or precursor material.

STATEMENT OF THE PROBLEM

The research conducted in the production of this work had the goal of developing and producing an acceptable IR window material, a ZnS-GaP nano-composite. The development of these composites was conducted in four definable sections.

1. Production of uniform, nanocrystalline ZnS powders and determining their sintering characteristics.
2. Production of GaP precursors for use in impregnating ZnS powders.
3. Formation of ZnS-GaP composites and determining their sintering properties and usefulness as IR window materials. (Figure 2)
4. Fabrication of IR windows from the nano-composite powders with subsequent testing for IR and mechanical properties.

Three different research groups collaborated in this effort with one member of each group contributing. Y. Han[10] acted as the coordinator and conducted all the ZnS synthesis, heat treatments, formation of the composites and some of the characterization. A. A.. Naiini[11] conducted all the production of GaP precursors as well as assisting in the formation of composites. My contribution, and the theme of this work, was providing Transmission Electron Microscope (TEM) characterization, enabling the team to evaluate the progress of the project. I also assisted in scanning electron microscopy (SEM), powder production and X-ray Diffraction (XRD). In order to present a coherent account of the entire process, work will be presented from all three of these research groups.

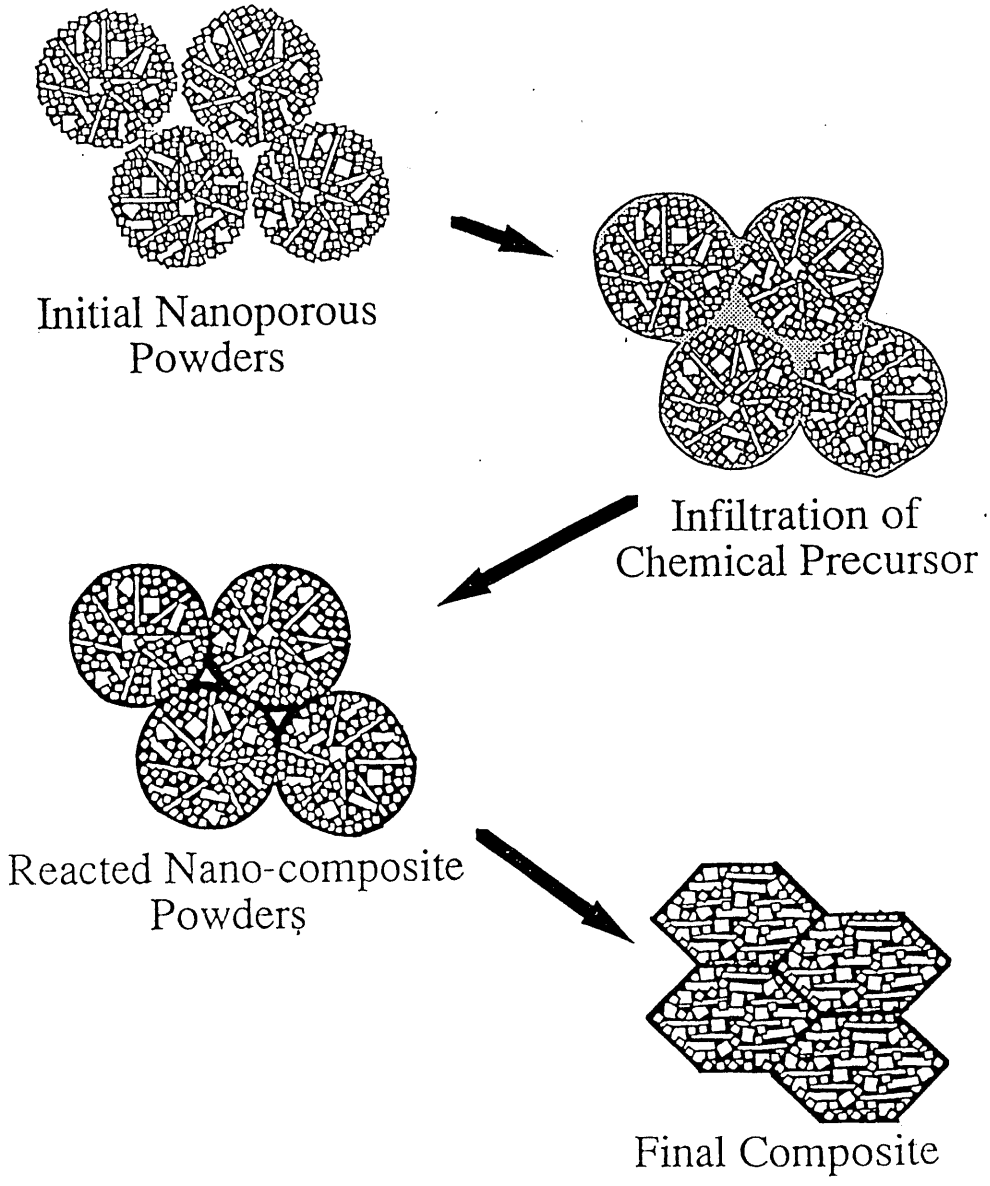

Figure 2. Conceptual design of nano-composite synthesis[10]

BACKGROUND

Formation of Nanocrystalline ZnS

The production of reliable and reproducible ceramic components for high technology application requires strict control over critical powder characteristics which include chemical homogeneity, low impurity levels, small particle size, narrow size distributions and freedom from agglomerates.[12] The conventional method for ZnS production is the passing of H_2S through a water solution containing Zn^{++} ions. Concentration gradients and stirring are inherent in this technique and result in very small irregular ZnS crystallites having a size distribution ranging from 25 to 200 nm.[13] This irregularity makes the conventional method unacceptable for the production of the highly uniform powders necessary for the fabrication of quality IR windows and so more precise methods of powder production are needed. A variety of methods have been proposed for obtaining small, uniform, unagglomerated powders. Among these methods, precipitation from aqueous solution are more common and provide better control over particle size and uniformity.[1]

The first mono-sized, spherical particles of ZnS were produced by complexing zinc ions with EDTA (ethylenedinitrotetraacetic acid, disodium salt) followed by precipitation by bubbling H_2S gas though the solution.[14] This method produced a mean particle diameter of 0.2 μm but in quantities too small to be useful. Later, Wilhelmy and Matijevic[15] employed thermal decomposition of thioacetamide (TAA) to prepare micrometer-sized spherical particles by first precipitating ZnS "seeds" (spherical submicron crystals) and aging them at elevated temperatures. A nearly identical method was employed by Willams et al.[13] producing similar spherical particles but differing in that their "seeds" were faceted single crystals.

More recently, several papers have been published by Celikkaya[9,16], still using TAA decomposition as basis, that relate the many variables, i.e., pH, ion concentration, temperature, etc., to properties of the ZnS powders, i.e., crystallite size, size distribution, morphology, etc. The experimental methods used by Celikkaya were adopted and used in the production of ZnS powders for this work.

Precipitation of zinc sulfide by thermal decomposition of TAA in acidic solution is known to proceed as shown in Figure 3 with the decomposition of TAA the rate limiting step.

Synthesis of GaP Precursors

Coates[17] and co-workers reported the preparation of $(Me_2GaPR_2)_n$ (R = Me, Et and Pr) by using alkane elimination from the reaction of trimethylgallium and dimethyl-, diethyl-, or diphenylphosphine. Cowley and Jones[18] employed a salt elimination method to prepare a number of GaP precursors from a mixture of lithium dialkylphosphide, $GaCl_3$ and alkyl lithium. For this work the precursors $[(t\text{-}Bu)_2GaP(i\text{-}Pr_2)]_2$ and $[(t\text{-}bu)_2GaP(i\text{-}Bu)_2]_1$ were formed and subsequently used to impregnate the ZnS powders. The precursors were formed by the reactions shown in Figure 4 with the final reaction occurring in a benzene solution. A detailed account of the production of the GaP precursors is given by A. A. Naiini.[19]

Formation of ZnS-GaP Nano-Composites

A conceptual diagram of the composite formation and final densification process can be seen in Figure 2. The impregnation is accomplished by dissolving the GaP precursor in Et_2O (ether) and then injecting it into an evacuated tube containing the ZnS powders. The precursor then infiltrates the nano-sized pores present within

$$H_2N\text{-}C(S)\text{-}CH_3 \xrightarrow{H_3O^+} H_2N\text{-}C(O)\text{-}CH_3 + H_2S$$

$$H_2S \overset{H_2O}{\leftrightarrow} HS^- + H_3O^+$$

$$HS^- \overset{H_2O}{\leftrightarrow} S^{=} + H_3O^+$$

Zinc nitrate or acetate : 0.05 M
Nitric or acetic Acid : pH=2.0
Thioacetamide : 0.4 ~ 0.8 M
Temperature : 70 ~ 80°C

Celikkaya and Akinc, J.Am.Ceram.Soc. **73**, 1990

Figure 3. General parameters and reactions for the formation of ZnS

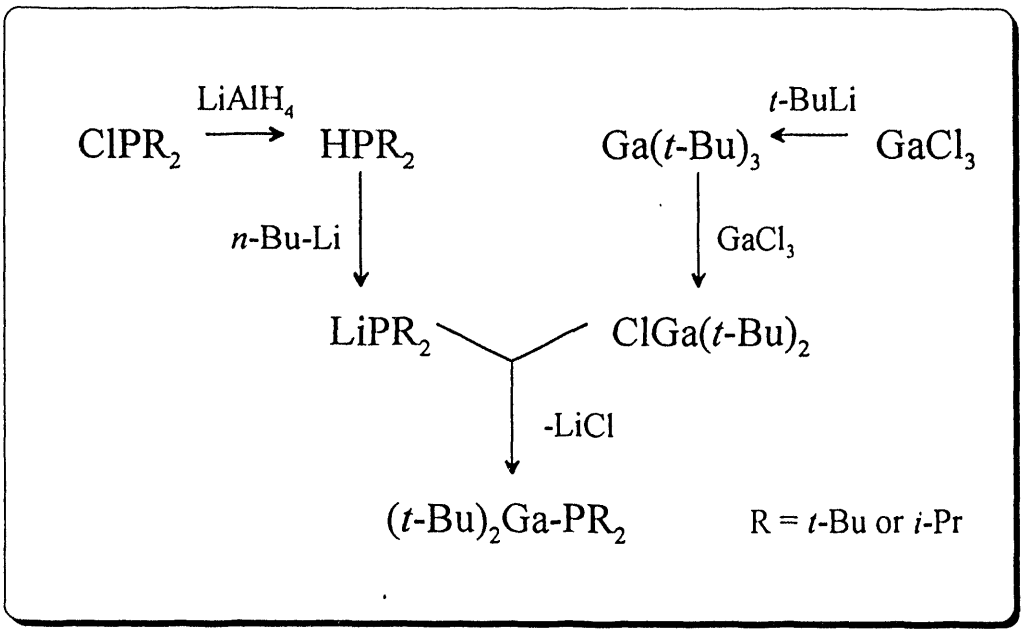

All reactions were carried out
in a double manifold vacuum line.

Naiini, Han, Akinc and Verkade, a manuscript submitted to Inorganic Chemistry for publication Dec. 1992

Figure 4. Equations governing the formation of GaP precursors

the ZnS powders. After removal of the Et_2O by slow evaporation at -22°C the entire batch is lowered into a pre-heated box furnace (Figure 5). Experiments on the precursor material showed that this quick heating (known as flash pyrolysis) converts the GaP precursor into cubic GaP by removal of the organic components, and it is believed that the same reaction occurs in the precursor material contained within the ZnS powders. The final product of this process is a ZnS powder impregnated on a nano-scale with GaP. The powders then can be processed by conventional methods into bulk forms.

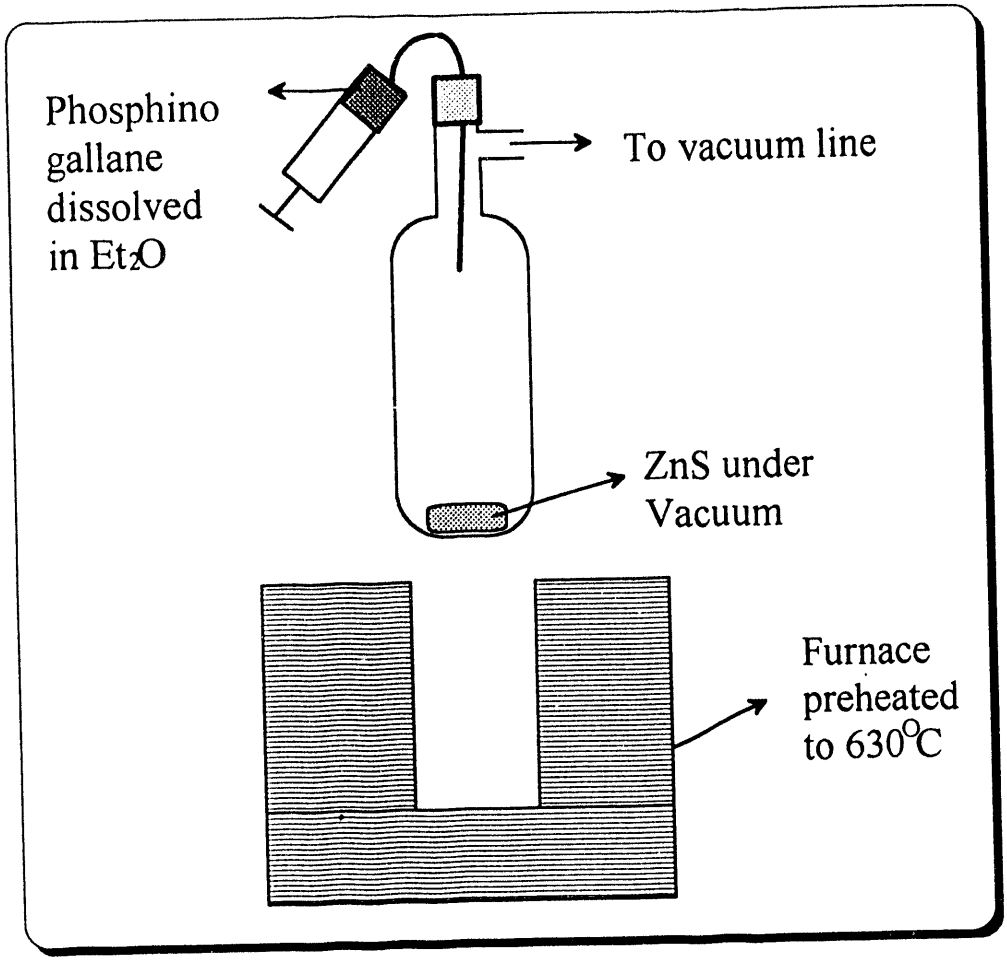

Figure 5. Experimental apparatus for the production of composites[10]

EXPERIMENTAL PROCEDURE

Production of ZnS

ZnS powders were prepared via homogeneous precipitation by the thermal decomposition of thioacetamide in acidic aqueous solutions. The zinc source for these reactions was zinc nitrate, zinc chloride or zinc acetate with a matching acidic partner (e.g. nitric acid with zinc nitrate). The equations and parameters for these reactions are shown in Figure 3. Each method shall hereafter be referred to by its zinc source, hence a reaction involving zinc nitrate in a nitric acid solution would be called the nitrate method. All three methods, nitrate, chloride and acetate, were used to fabricate various batches of ZnS with the total number of batches exceeding 60. Each method follows a similar experimental procedure, based on earlier work by A. Celikkaya[9,16], and modified through further experimentation. Most of the powder was obtained from Y. Han[10] with the only exception being batch #56 which was prepared using the acetate method by myself. The following is a detailed account of the acetate method which produced more consistent, more reproducible results than the other methods. This extensive account is intended to show the great precautions necessary to produce top quality ZnS particles and the amount of time needed to produce useful quantities.

Acetate method

A clean beaker is first washed with a concentrated solution of HCl with subsequent washings with de ionized water and acetone. After a 15 minute drying period in a 120°C oven a compressed air spray is used to remove any remaining particulate matter in the beaker. These elaborate cleaning techniques proved

necessary to the production of consistently mono-sized, nanocrystalline, dispersed powders.

Two graduated cylinders are then cleaned in a similar manner and then rinsed with the Zn^{++} source, zinc acetate, in a 1.0 M concentration. 80 ml of the 1.0 M Zn^{++} source is then measured out in one cylinder and 20 ml of 0.05 M HCl in the other. These amounts of Zn^{++} and HCl are then combined with 200 ml of de-ionized water in the previously cleaned beaker.

A pH meter is then cleaned with de-ionized water and calibrated with pH 4 and 7 standards. Now 300 ml of acetic acid is added to the previous mixture and its pH measured. Additional acetic acid and de-ionized water are added alternately until at least 50 ml of acetic acid is added and the pH is exactly 2.00. After this exact pH is achieved a cover is placed over the beaker to prevent any evaporation or excessive contamination of the prepared solution which now contains 80 ml of Zn++, 20 ml of HCl, 350 ml of acetic acid and about 325 ml of de-ionized water. The covered beaker is then placed in a controlled water bath which is kept at approximately 80°C.

An amount of reagent grade thioacetamide (TAA) (Aldrich Chemical Co., Milwaukee, WI) equaling 48.08 grams is weighed (in a hood due to its carcinogenic nature) and added to the covered beaker in the water bath, accompanied by a strong stir. No further agitation is used and the cover on the beaker is replaced. After large scale nucleation occurs, usually within 3 minutes, the solution takes on a bluish hue and is then allowed to "age" for approximately 3 hours. This aging allows the slow growth of the ZnS powders and increases the yield, the growth being slow due to the low concentrations of each reagent in the reaction.

The solution is then removed from the water bath and quenched in an ice bath to prevent further nucleation and growth. The solution is then centrifuged at 6000 rpm for approximately four hours. This time consuming step is necessary due to the great stability of the suspension of ZnS particles in their host liquid. After centrifuging the host liquid is decanted, leaving the ZnS particles agglomerated at the bottom of the centrifuge container. An amount of 0.002 M HCl is added and the container is shaken to re-suspend the ZnS particles using an ultrasonic disrupter for three minutes. This ensures good dispersion and adequate washing of the particles for any contaminants. This "washing" procedure is then repeated twice with five-hour centrifuges instead of the initial four. A final two washings using acetone instead of HCl and only two hour centrifuges completes the washing process.

After the final wash the centrifuge bottles are decanted and then dried in an oven at 120°C for 10 minutes to drive off any remaining acetone. The dried powder is then weighed and compared to its theoretical yield of 3.8 grams. A final purification step involves heating the powder under a continuous vacuum of 10^{-6} torr at 400°C for five hours. This heating is intended to drive off any surface contaminants that may remain. A final check of the quality of the powder is conducted by examination in a Scanning Electron Microscope (SEM).

More than 60 batches of ZnS were produced with varying degrees of success in regards to yield, morphology and purity. Two examples are shown in Figure 6. Only those batches which were of the highest quality were used in the subsequent experiments with the remaining batches being discarded. Batch numbers were used throughout the experiments to track the success of the various methods. Batches #18, 20, 24 were prepared by the nitrate method, #37 by the chloride method and #56 by the acetate method.

Production of GaP Precursors

All GaP precursor production was carried out by A. A. Naiini.[11,19] The compound {[(t-Bu$_2$GaP(i-Pr)$_2$]$_2$} was formed by adding to a mixture of 0.56 g (4.5 mmol) of LiP(i-Pr)$_2$ and 1.00 g (4.5 mmol) of ClGa(t-Bu)$_2$ about 25 ml of dry, degassed benzene. The mixture was stirred overnight at room temperature and then filtered. Benzene was removed under vacuum to give 1.1 g of white product in 80% yield which was purified by sublimation at 90°C at 5 x 10^{-3}. An analogous procedure was used to form [(t-Bu)$_2$GaPi-Bu]$_1$ with LiP(t-Bu)$_2$ replacing LiP(i-Pr)$_2$. A detailed explanation of the procedure is available.[19]

Heat Treatment of ZnS powders

To study the sintering and grain growth behavior of the ZnS powders samples were heat treated in sealed quartz tubes at 500, 600, 700, 800 and 900°C for at least 20 hours with the resulting samples being examined with X-ray diffraction (XRD), Infra-Red Absorption, Scanning Electron Microscope (SEM) and Transmission Electron Microscope (TEM) methods. I was responsible for all TEM investigation and most of the SEM. The results of these examinations are shown later in this work. All heat treatments, X-ray and infra-red studies were performed by Y. Han.[10]

Compacts of ZnS powders were also made to facilitate the examination of the close packed sintering properties as well as densification behavior. The compacts were made by pressing 20 mg of ZnS #18 powders in a uniaxial press at 500 MPa in a 0.32 cm diameter double-acting stainless steel die. A cold iso-static press was then used to do the final forming of the pellets at approximately 340 MPa. These pellets

were then heat treated in sealed quartz tubes at 500, 600, 700, 800 and 900 ℃ for at least 20 hours. Each pellet was then broken into at least two pieces, one of which was mounted in Bakelite for polishing and the other kept intact as a fracture surface specimen. The mounted pellet was subsequently polished on polishing cloths 15 minutes using 1μm, 0.5 μm and 0.25 μm diamond compounds each with intermittent washings in methanol. An SEM investigation of both the polished and fracture samples was conducted and is shown later in this work.

A second series of ZnS compacts was fabricated to examine how the sintering and densification properties of the nanocrystalline ZnS compares to that of commercial ZnS. Pellets of ZnS #18 and ZnS from Fisher Scientific Co. were formed by dry pressing 200 mg uniaxially at 34 MPa in a 0.95 cm double acting stainless steel die followed by iso-static pressing at 340 MPa. These compacts were then sealed in quartz ampoules and sintered at 600 and 700℃ for at least 20 hours. Subsequent SEM investigations on fracture samples are shown later in this work. Densities of the green and sintered pellets were measured by employing Archemedes method.[10]

In-situ heating of ZnS

Real time heat treating experiments were carried out on ZnS #24 using a Gatan heated stage and the Phillips CM30 TEM. These experiments were intended to mimic the previous heat treatments and so facilitate a greater understanding of the grain growth and sintering mechanisms of the ZnS. Runs were made at 500, 600, 700 and 800℃ and lasted 20 hours each. Due to the constant motion of the sample during heating and the drifting of the sample during the time held at temperature it

was impractical to take normal micrographs. A digital camera and VCR were used to record each experiment with reproductions made using a thermal printer.

Formation of Composites

Nano-composites of ZnS and GaP were formed using the apparatus displayed schematically in Figure 5. All composite formation was carried out by Y. Han[10] and A. A. Naiini[11], and I was responsible for microstructural examination. The following procedure is included for the sake of completeness .

The experimental apparatus is loaded with one gram ZnS which is dried, under constant vacuum, at 350°C for 5 hours. After a cool down period the unit is evacuated down to 0.01 torr after which 500 mg of a phosphino gallane dissolved in 15 ml Et_2O is injected through a septum. A mixture of CCl_4 and liquid N_2 is then used as a slush-bath to bring the sample temperature down to -22°C. This temperature is then maintained for 30 minutes to evaporate the Et_2O (ether) very slowly so as to prevent loss of the sample. The loaded unit is then lowered into the preheated box furnace which brings the sample to 600°C in 2 minutes. This quick heating (flash pyrolysis) causes the organic components on the GaP to evaporate. After 30 minutes at 600°C the apparatus is then removed and cooled to room temperature.

Eight composite batches were made during this investigation with initial ZnS powders being formed from both the nitrate and acetate methods and target GaP concentrations ranging from 4 to 24 wt%. These composites are hereafter referred to by their batch number and target wt% GaP. X-ray Diffraction (XRD), SEM and TEM methods were used to characterize these powders as well as chemical analysis the results of which are shown later in this work.

Heat Treatment of Composite Powders

To study their sintering and grain growth behavior the composites were heat treated in a manner identical to that used on the ZnS powders. Composite powders were heated at 500, 600, 700, 800 and 900°C for at least 20 hours in sealed quartz tubes with subsequent examination by XRD, SEM and TEM techniques as shown later in this work. Chemical analysis was carried out on these heated samples using Inductively Coupled Plasma (ICP) techniques with the results shown later.

In-situ TEM heat treatments were carried out on the composites using an identical procedure as used for the ZnS powders. These experiments were intended to reveal the origin and mechanism of formation of large single crystals in heat treated composite samples examined previously. Runs at 700, 800 and 900°C were carried out on composites 004, 006, 007 and 008 with the results from composite 006 (4 wt% GaP) shown in the later part of this work.

Preparation of SEM Samples

All powder samples were prepared in the following manner. A small amount of powder is placed in a mortar and ground for approximately 5 minutes in a methanol solution to break up any agglomerates. A carbon stub 1 cm in diameter is then prepared by first sanding it flat and then affixing a 3 mm disk of aluminum foil to it using carbon paint. The powder suspension in the mortar is then deposited onto the aluminum disk using an eyedropper and allowed to dry. Carbon paint is used to ensure electrical contact between aluminum foil disk and the edge of the carbon stub. Finally, the entire sample is coated with gold in a Hummer Sputter Coater. This elaborate amount of preparation was found to be necessary due to

charging problems resulting from the poor electrical conductivity of the samples examined.

Fracture samples are obtained by striking the specimen, usually a small pellet, with a pick, causing it to break into two or more pieces. A suitable piece is chosen and mounted on a carbon stub with the preserved fracture surface facing upward. The sample is affixed to the stub by carbon paint. Finally the entire assembly is coated with gold in a Hummer Sputter Coater.

Polished samples are fabricated from the remaining pieces of the specimen pellet after the fracture sample is removed in the following manner. A fragment is mounted in Bakelite and subsequently polished with 1, 0.5 and 0.25 micron diamond slurry for 15 minutes each with intermittent washings with methanol. After drying for 2 hours the samples are then coated with gold in a Hummer Sputter Coater.

All SEM samples are kept in a dry box until examined to prevent excessive contamination and degradation by moisture.

Preparation of TEM Samples

All TEM samples were fabricated using carbon coated 3 mm copper grids manufactured by Ted Pella Co. A small amount of the sample is placed in a mortar and ground for 5 minutes in a methanol solution. This suspension is then deposited onto the carbon coated grid with an eyedropper and allowed to dry. The samples were then kept in a TEM sample holder in a dry box until needed for the same reason as for the SEM samples.

RESULTS AND DISCUSSION

Production of ZnS Nanocrystalline Powders

The nitrate method for the production of ZnS powders proved to be both predictable and reliable in the production of mono-sized spherical powders, as seen in Figure 6a. XRD of powders formed by this method showed an initial average grain size in the 8 nm range, Figure 7 and Table 3, with the predominant phase being cubic (Figure 7 and Table 2). Only when the batch parameters deviated significantly from those displayed in Figure 3 did the morphology differ from the ideal. The only problem with powder derived from the nitrate method is that it tended to have excessive contamination, degrading its Infra-Red (IR) characteristics, Figure 8. These surface species cause absorption in the 8-12 μm range, precisely the area of interest.

Production of ZnS using zinc chloride as the zinc source, the chloride method, proved too erratic and unpredictable for the formation of useful quantities of powders. Frequently samples like that shown in Figure 6b would result with continuous size distributions and frequent agglomeration. Considerable work was done by Y. Han[10] in an effort to pin down the correct parameters so that consistently high quality powder could be obtained. This effort was primarily because the surface subspecies are not as much of a problem in the chloride (Figure 9) as the nitrate. Eventually this system was abandoned due to its erratic behavior.

The final method employed in the production of ZnS powders was that of using zinc acetate as the zinc source, the acetate method. This system proved extremely consistent and provided the highest quality powders with respect to grain size and morphology. An XRD investigation of an acetate powder shown in Figure 20 shows an average initial grain size of 8 nm. The one problem with the acetate method is the excessively stable suspension formed in the initial production of

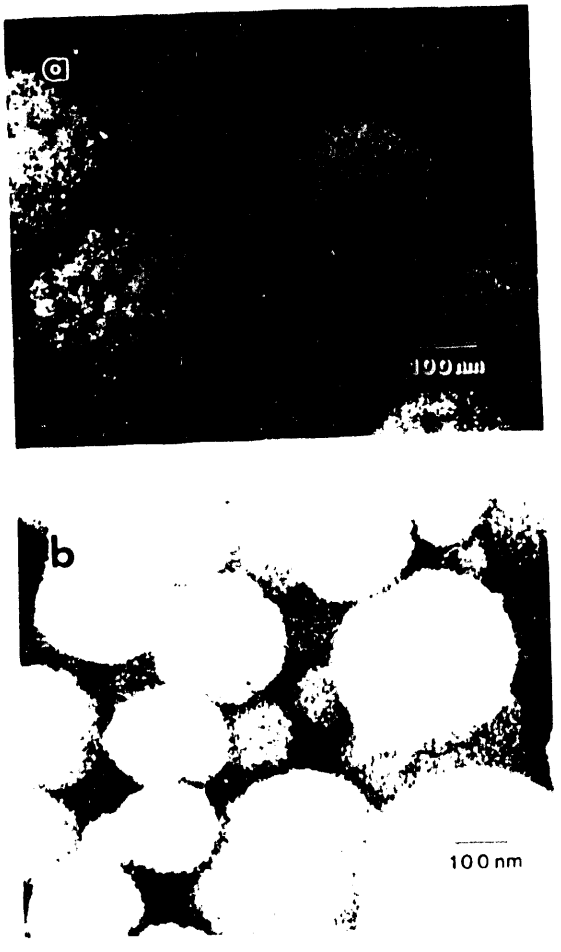

Figure 6. SEM secondary electron image, 15 kV, 8 mm WD
as-prepared ZnS powders[10]
a) ZnS #20 - nitrate method b) ZnS #37 - chloride method

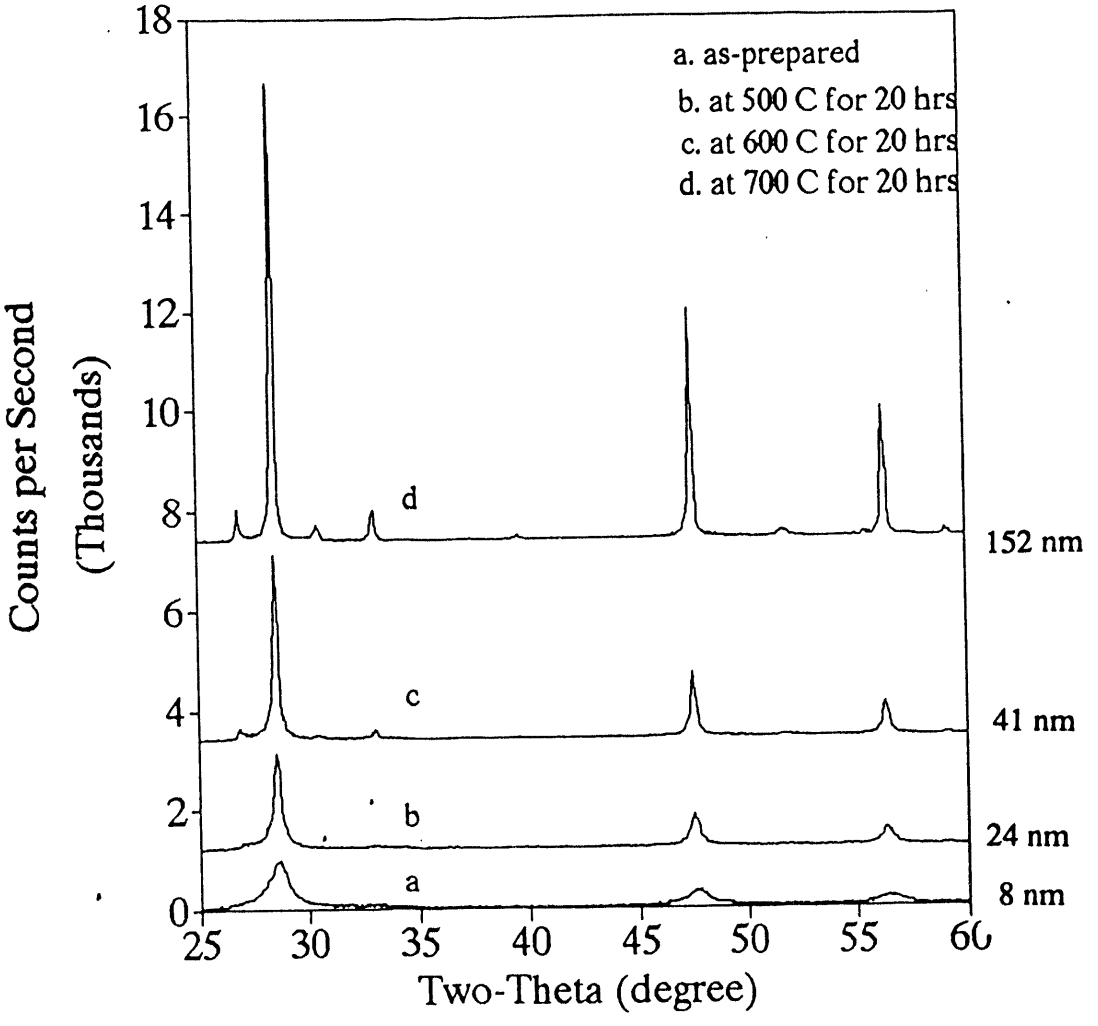

Figure 7. X-ray diffraction pattern for heat treated ZnS samples[10]

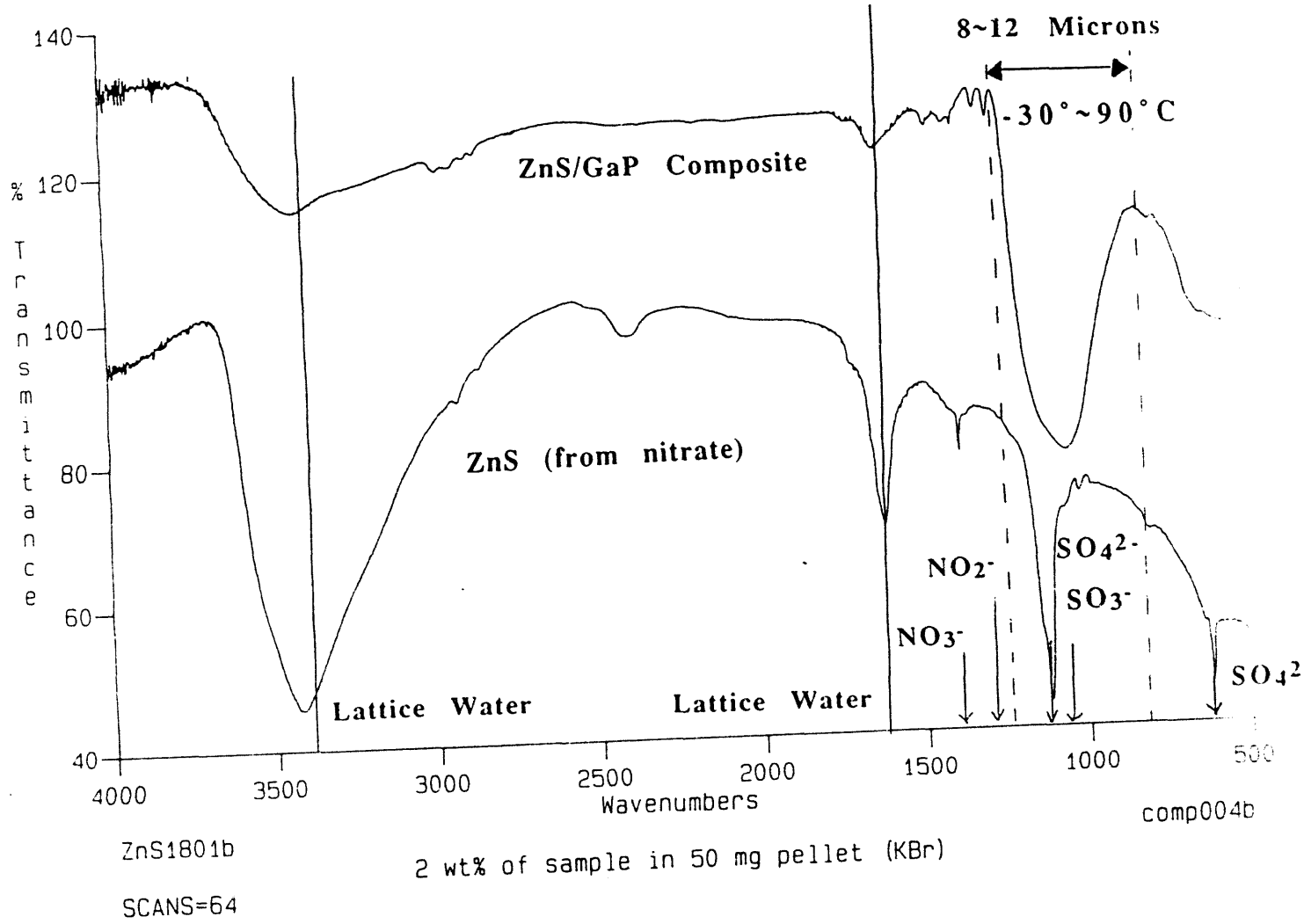

Figure 8. Infra-red absorption of ZnS samples prepared by the nitrate method and composite 004 that used this powder as its initial material[10]

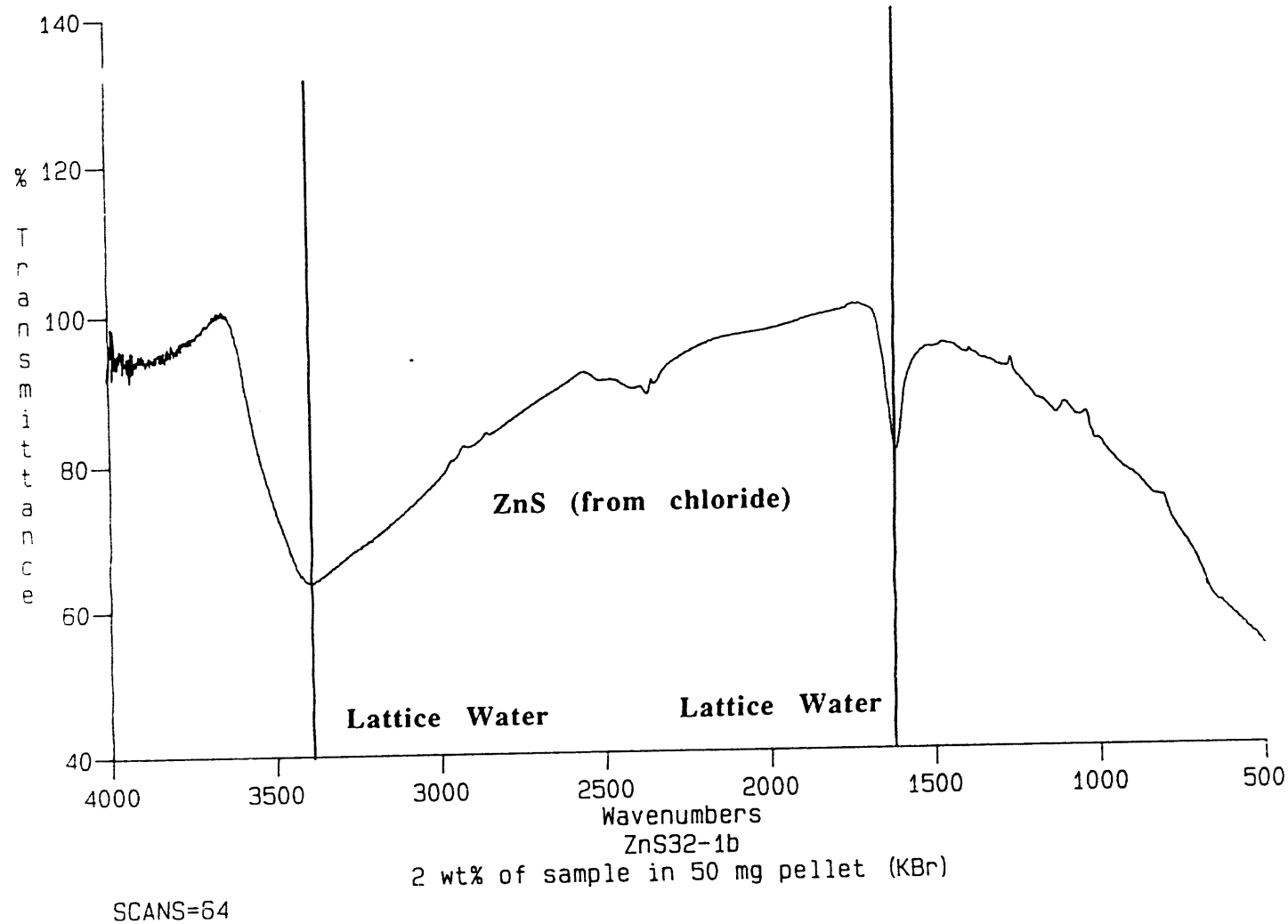

Figure 9. Infra-red absorption for ZnS prepared by the chloride method[10]

powders. This necessitated extremely long centrifuging times and so greatly slowed the production schedule. Using the optimal conditions in Figure 3 and the procedure detailed previously it was only possible to produce approximately 3.5 g of ZnS powder in a 24 hour period. Efforts were made to increase the batch size but with each attempt the reaction became more erratic and produced poor quality powders. This method was used to produce large quantities of powder for use in later composite formations.

Heat Treatment of ZnS Powders

The numerous heating experiments carried out on the various ZnS batches were intended to give an indication of the sintering and grain growth properties of these new materials as well as demonstrate their nanocrystalline nature. Runs were made at 500, 600 and 700°C as detailed in the experimental procedure section of this work.

The resulting heat treated samples were first examined with X-ray diffraction (XRD) to check for the crystallinity, average particle size and predominant phase. These runs yielded the scans shown in Figure 7. Examination of these scans confirms that the sphalerite (cubic) phase is predominant in each sample and that the average grain size increases with temperature, Table 3. Grain growth proved to be the dominant sintering mechanism in the ZnS powders examined.

Scanning Electron Microscope (SEM) micrographs were taken of each heat treated sample and are shown in Figure 10 along with their complimentary TEM micrographs in Figure 11. Micrographs of as-prepared powder shown in Figure 10a confirm the nanocrystalline nature of the powders and their general morphology of submicron spherical powders of uniform size and shape. Nano-size porosity was

Figure 10. SEM secondary electron image, 15kV, 8 mm WD
Zn #20 powder heat treated at several temperatures[10]
a) as-prepared b) 500 C for 20 hours
c) 600 C for 20 hours c) 700 C for 20 hours

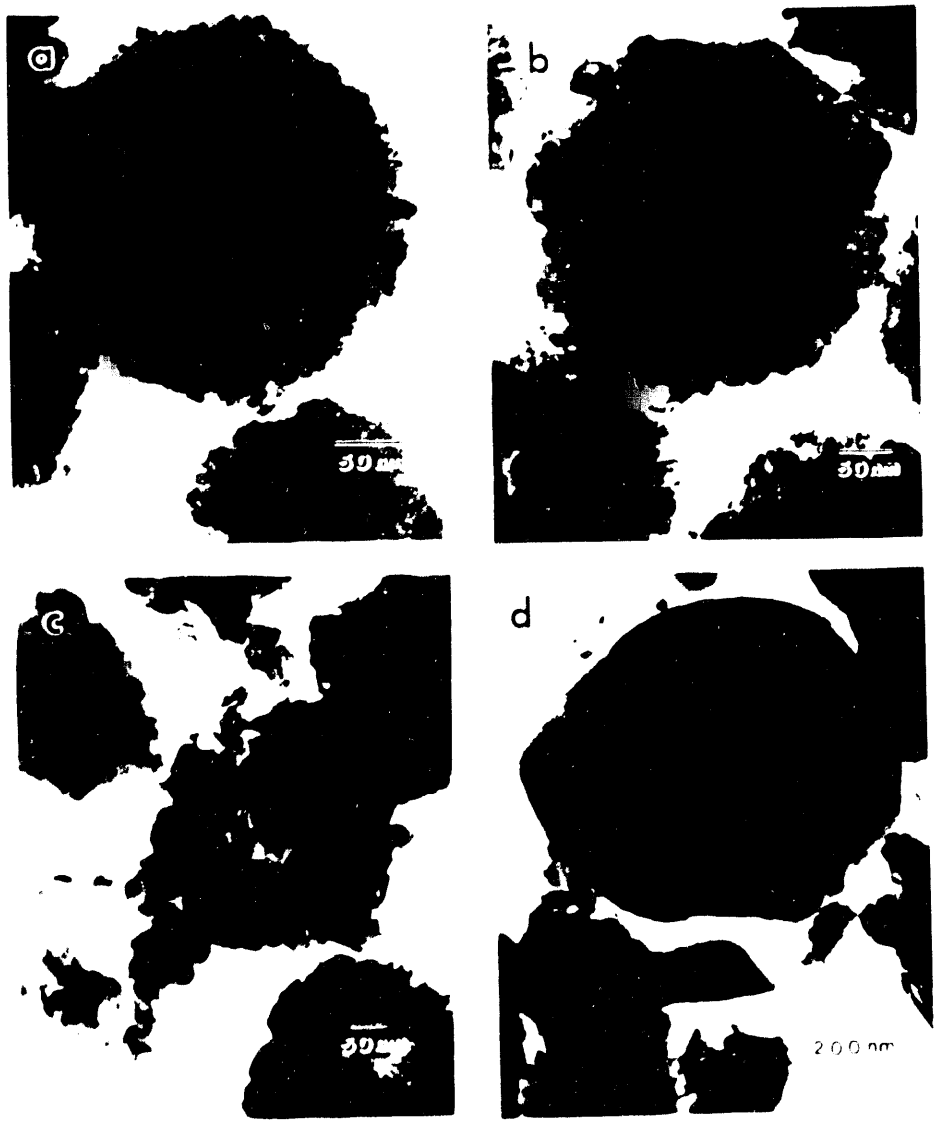

Figure 11. TEM bright field image, 300kV
ZnS #20 powder heat treated at several temperatures
a) as-prepared b) 500 C for 20 hours
b) 600 C for 20 hours d) 700 C for 20 hours

observed in as-prepared powders, as shown in Figure 11a, as well as an almost perfect spherical morphology. Coarsening of nano-crystallites was observed at temperatures as low as 500°C and inter-particular diffusion (necking) started to occur at 600°C , Figures 10b, c and d. At 700°C (Figure 10d), the initial morphology of the powders were completely lost and particles with a few micrometers in size were observed. Average crystallite sizes measured from these micrographs were 14^{+}-3 nm, 42^{+}-4 nm, and 66^{+}-5 nm for as-prepared powders and powders heat treated at 500°C, and 600°C, respectively. These values somewhat contradict the values obtained through XRD and are contrasted with them in Table 3. The differences in these values may be explained in that the XRD method provides an average measure of the grain size for a large number of powders. The XRD results, therefore, represent a true grain size measurement for a bulk sample. Thus, either the XRD samples contain additional nanocrystalline material not present in the powders, or the size of the grains in the interior of the powders is smaller than those at the edges. Since no additional nanocrystalline material separate from the powders was observed in the TEM, there must be a variation in grain size either from powder to powder or within the powders themselves. Since the SEM investigations showed all of the powders to be remarkably uniform in grain size on the surface of the powders, the most likely explanation for the descrepancy between the XRD and the TEM results is that the grain size is smaller in the center of the powders than at the surfaces. In the TEM only those grains near the edge of the powder can be measured accurately. This is due to the overlapping of grain boundaries in the interior of each particle, making it impossible to differentiate grains and obtain an accurate grain size measurement from this region. Thus, a change in grain size may be present but remain undetected by TEM. This

hypothesis appeared valid given the "hollowing out" of the spherical powders observed upon heat treating. Powders heat treated at 500°C consisted of essentially spherical particles that maintained the initial particle sizes, however, the individual particles showed hollow centers and significant grain growth within the particles (Figure 11b). In the 600°C sample, grain growth continued, maintaining and expanding the hollow center (Figure 11c). At 700°C massive single grains were developed as the result of sintering (Figure 11d).

This "hollowing" of each spherical powder, discovered solely through TEM investigation and shown in Figure 11, proved to be undocumented by any other previous work in ZnS. Subsequent in-situ heating experiments revealed this to occur in the first few hours of the heating cycles.(Figure 12) Presumably this hollowing involved the transport of interior material to the sphere exterior. If, as hypothesized, the interior grains of each sphere are smaller than those on its exterior, surface energy effects will cause diffusion of material from the smaller to larger grains. If the overall size of the sphere does not change (and it did not as measured from TEM micrographs) this diffusion would leave the interior hollow.

This "hollowing out" was seen as proof that the spheres are not sealed and are in fact quite porous. The large degree of porosity proved favorable to the formation of composites (conducted in the latter portion of this study) in that the composite precursor material easily penetrated the spheres.

Another possible explanation for the "hollowing out" behavior is that the interior grains are small enough to have their melting point significantly depressed.[6] This depression could enable the interior grains to melt at temperatures equal to those used during heat treatment experiments. The molten ZnS could then move very quickly to the edges of the particles. Significant movement was seen inside

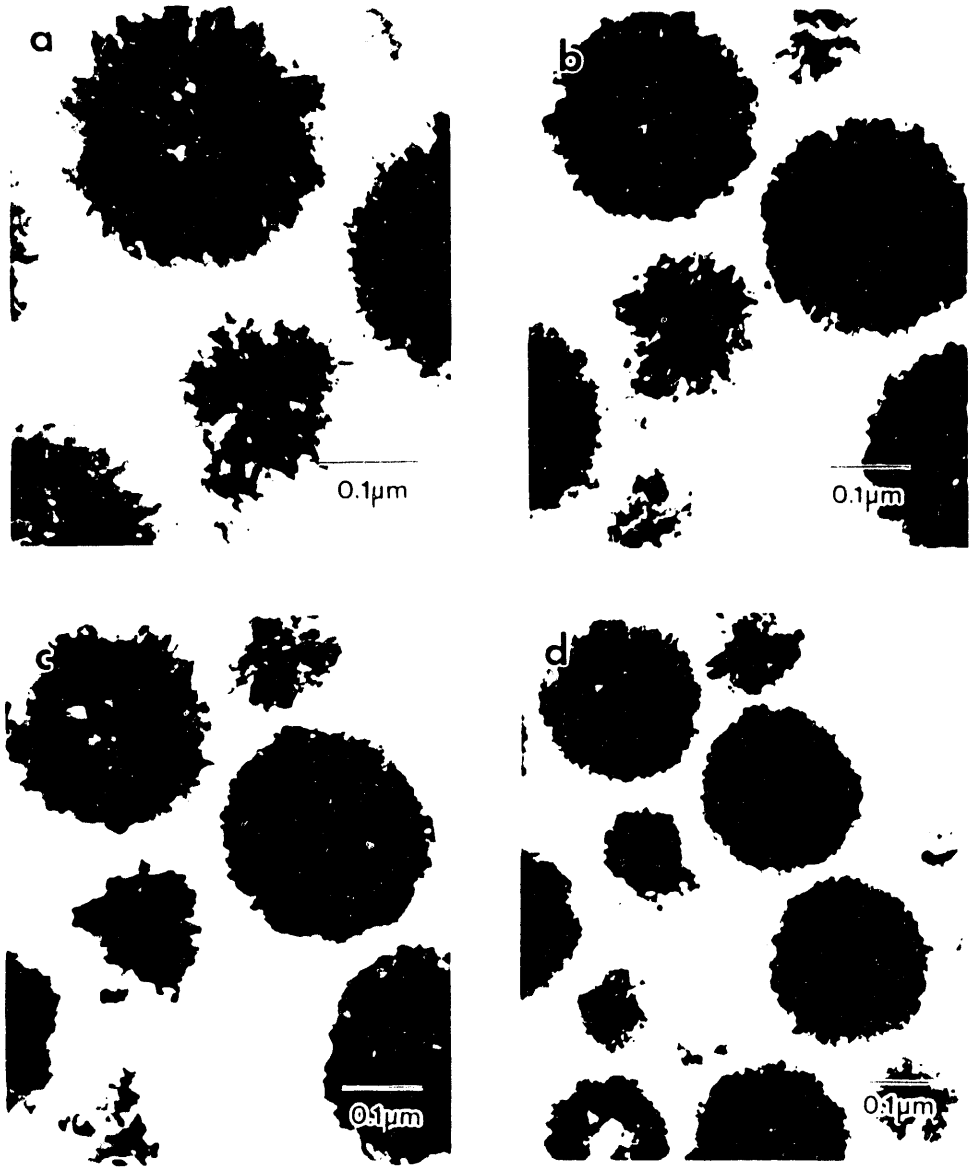

Figure 12. TEM bright field images, 300 kV
in-situ heat treated ZnS #24 showing "hollowing"
a) 600°C for 0 hours b) 600°C for 1 hour
b) 600°C for 4 hours d) 600°C for 8 hours

observed particles recorded during a run at 700°C although it is difficult to say positively whether this was indicative of melting or of mass transport via rapid diffusion. Differential Thermal Analysis (DTA) was performed on several ZnS powder with inconclusive results.[10] The small amount of material melting would produce a small endotherm which may have been lost in the background.

Heat Treatments of ZnS Pellets

Two series of compacts were made to study sintering and densification of ZnS as a function of temperature. The first series was to study the thermal behavior of the nanocrystalline ZnS powders produced for this study. The second series was a comparative study of compacts made from the nanocrystalline ZnS of this study and compacts made from commercially available ZnS powders. These compacted samples give a more accurate representation of ZnS behavior in a form that might be used for an actual IR window.

The first series was compacted as detailed in the procedure and heat treated at temperatures ranging from 600 to 900°C. The fracture samples obtained from these heat treatments were examined with the SEM and the results shown in Figures 13-15. The as-prepared sample shown in Figure 13a, b shows the nanocrystalline nature of both the interior and exterior of the spheres as seen in the fractured particle in the center. The interiors of these particles differ from those seen by Williams[13] and Wilhelmy[15] in which they observed solid cores of considerable size. At 600°C, the surface of the pellet underwent a significant degree of grain growth and sintering resulting in a submicron size microstructure. As the temperature increased, grain growth became more significant, and large pores formed. The spherical morphology of the individual powders is maintained until temperatures

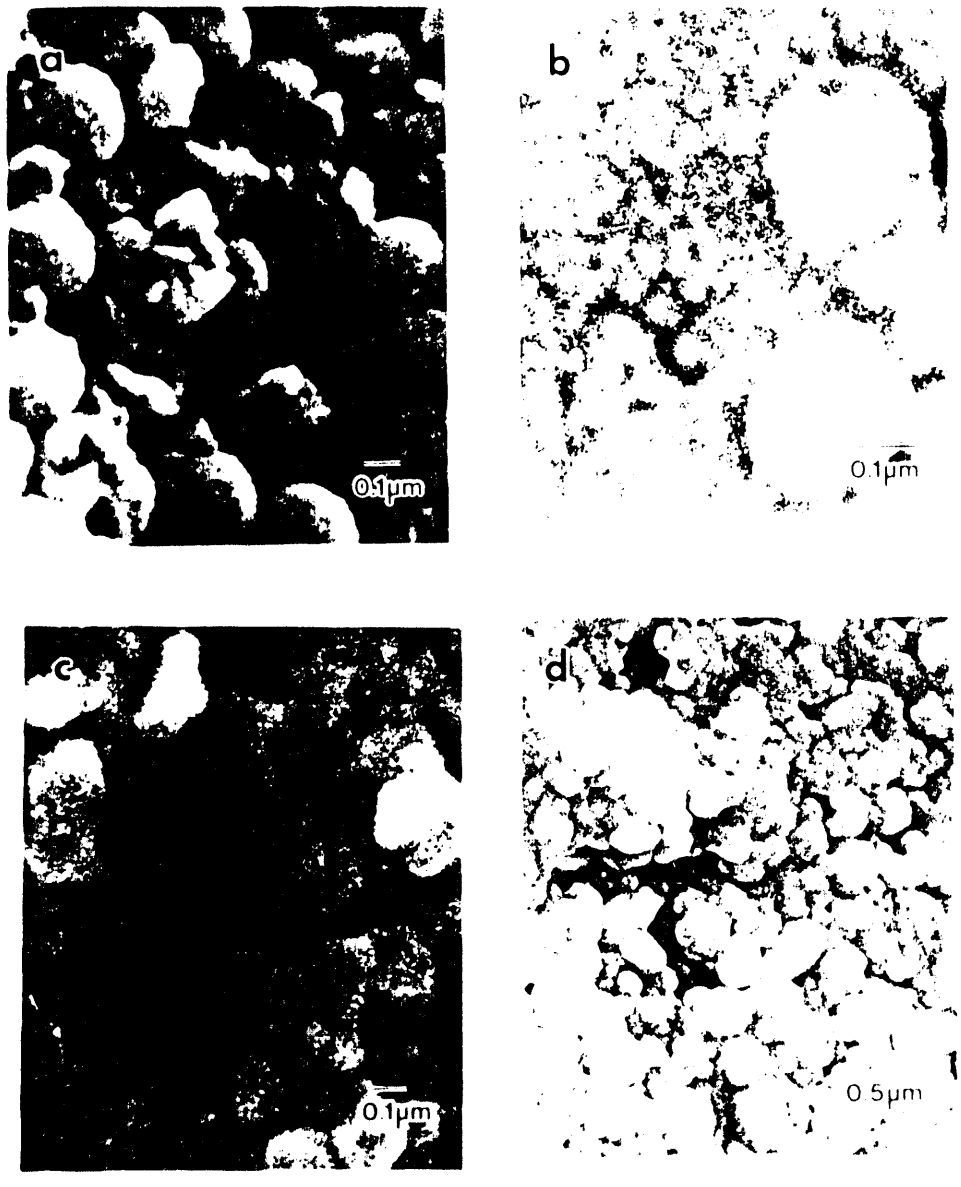

Figure 13. SEM secondary electron images, 15kV, 8 mm WD
ZnS #18 compacts, cip'd and sintered at several temperatures
a) as-prepared/fracture b) as-prepared/polished
c) 600°C for 20 hours/fracture d) 600°C for 20 hours/polished

Figure 14. SEM secondary electron images, 15kV, 8 mm WD
ZnS #18 compacts, cip'd and sintered at several temperatures
a) 700°C for 20 hours/fracture b) 700°C for 20 hours/polished
c) 800°C for 20 hours/fracture d) 800°C for 20 hours/polished

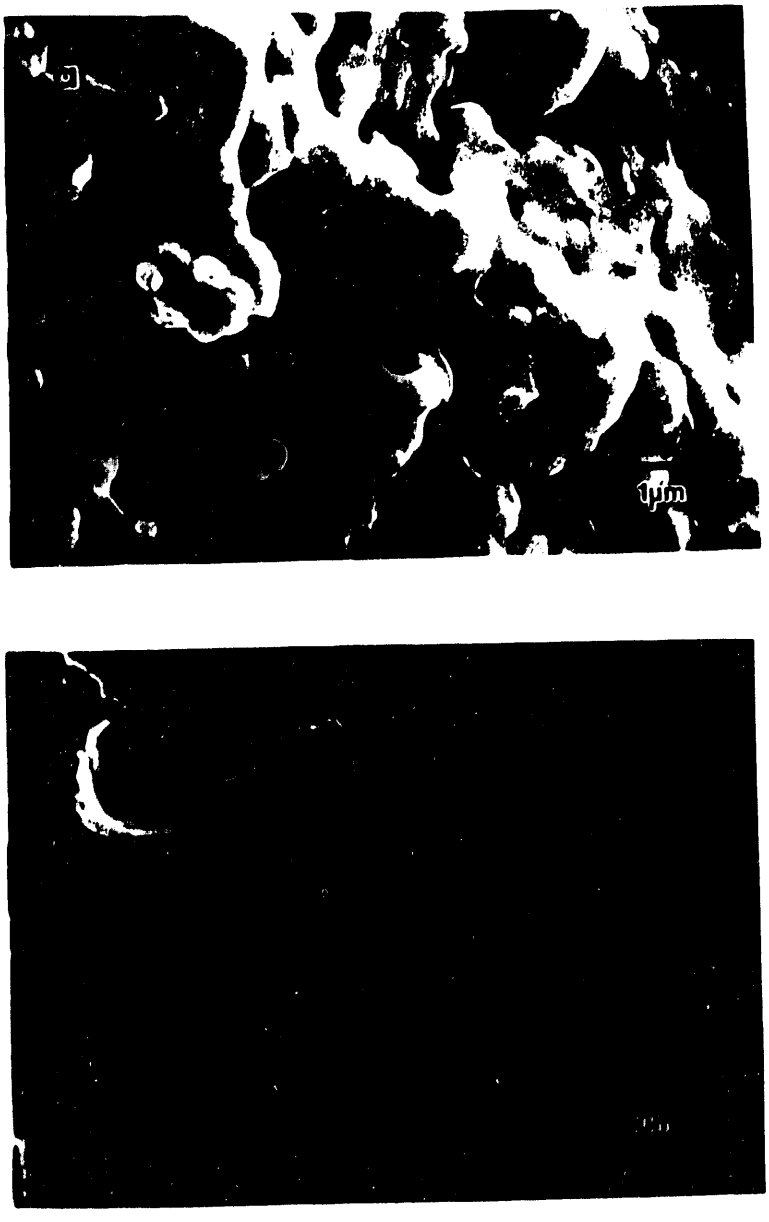

Figure 15. SEM secondary electron images, 15 kV, 8 mm WD
ZnS #18 compacts, cip'd and sintered at 900°C
a) 900°C for 20 hours/fracture b) 900°C for 20 hours/polished

above 700 °C with a total breakdown at 900°C. These findings are consistent with the previous powder heating experiments and in-situ experiments of this study.

Polished samples of the heat treated ZnS compacts show similar grain growth results to that shown in their complimentary fracture samples and are shown in Figures 13-15. However, the overall morphology of the powders, does differ. The fracture samples show intact spheres while the polished samples show a continuous body of nano-crystals (Figures 13-14). Only at 900°C do the morphologies of the complimentary samples agree (Figure 15). The appearance of the polished samples is believed due to the polishing process itself. During polishing the individual spheres are apparently broken and the smaller grains are distributed evenly over the surface of the sample, filling the gaps between the remaining spheres and giving the appearance of a continuous body. This "smearing" indicates that the spherical powders easily fracture and that the bond strength between grains is low. This behavior would be expected if the grains have significant porosity at the grain boundaries as believed.

To determine whether nanocrystalline ZnS has superior sintering properties to that of commercially available ZnS a series of compacts were fabricated and heat treated at 600 and 700°C. These temperatures were chosen because the first indication of inter-particular sintering was seen at these temperatures.

Fracture samples from these compacts were examined using the SEM with the results shown in Figures 16 and 17. Only fracture samples were examined. The as-prepared sample of the commercial powder, which differed in both grain size and morphology from the nanocrystalline ZnS, consisted of irregularly shaped, submicron, single grain particles of varying sizes. At both 600 and 700°C the two powders behaved similarly with respect to sintering and morphology changes. This

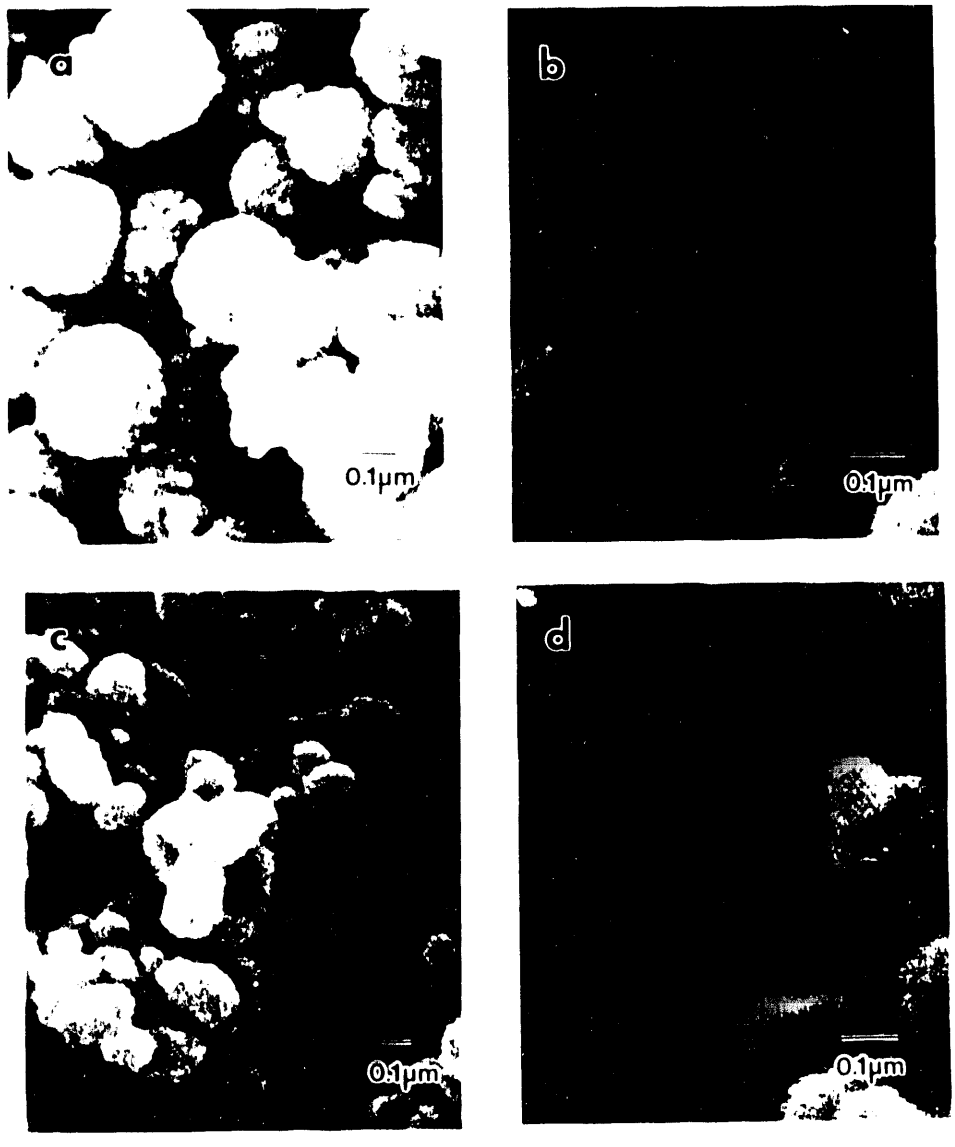

Figure 16. SEM secondary electron images, 15kV, WD 8 mm, all fracture samples commercial and ZnS #18 compacts, cold isostatically pressed (cip'd)
a) ZnS #18 as-prepared b)ZnS #18 as-prepared
c) commercial ZnS as-prepared d) commercial ZnS as-prepared

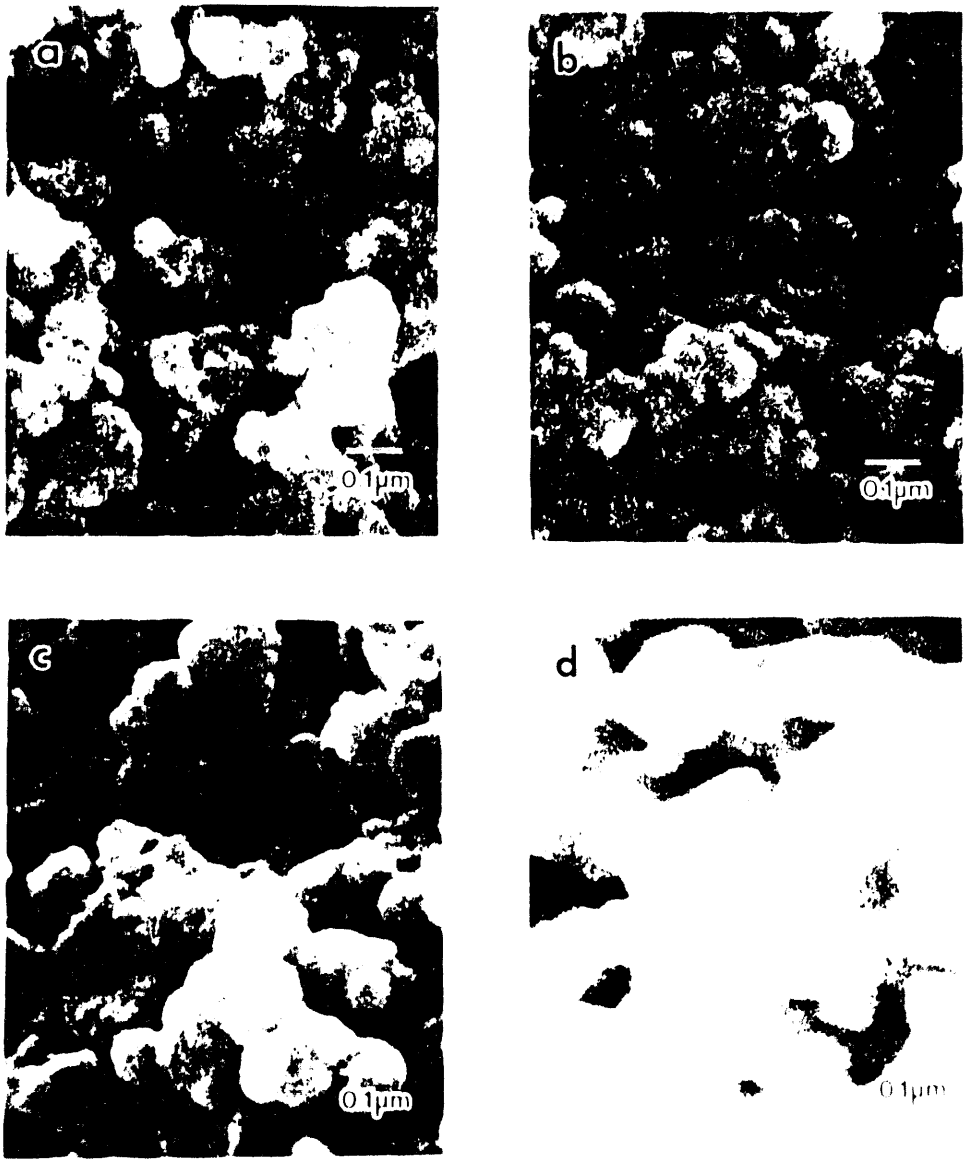

Figure 17. SEM secondary electron images, 15 kV, WD 8 mm, all fracture samples commercial and ZnS #18 compacts, cip'd and sintered at several temps
a) ZnS #18 600 C for 20 hours b) commercial ZnS 600 C for 20 hours
c) ZnS #18 700 C for 20 hours d) commercial ZnS 700 C for 20 hours

result is unexpected due to previous work showing that nanocrystalline material should have superior sintering characteristics.[8] The commercial powders' large size distribution (Figure 16c and d) enabled it to have a higher green density and subsequently more intimate contact than the uniform ZnS #18. This is in contrast to the point-to-point contact of the nanocrystalline spheres and the poor bonding of the grains within the spheres of ZnS #18. Under hot press conditions the nature of the nanocrystalline ZnS and the tendency of the powders to fracture should enable more intimate granular contact, resulting in better sintering and densification than for the commercial.

Significant porosity was measured in all the compacted samples, the measurements being made using Archemedes method. Pellet densities were found to be from approximately 56 to 60% of theoretical over the range of temperatures. The persistent porosity indicates that additional steps need to be taken for full densification of any ZnS body. A logical step would be to introduce hot pressing instead of the normal heat treatment or, if that is unsuccessful, hot iso-static pressing.

Formation of GaP precursors

Production of the GaP precursors was conducted by A. A. Naiini with the results being available.[11] Briefly, the reaction of an equimolar amount of t-Bu_2GaCl and i-Pr_2PLi or T-Bu_2PLi in benzene produced volatile $[(t\text{-}Bu)_2GaPR_2]_x$ wherin R=i-Pr, x=2 (compound 1) and R = t-Bu, x=1 (compound 2). Compound 1 was obtained as a white solid which can be sublimed at 90-95°C at $5x10^{-3}$ torr, while compound 2 isa low-melting, yellow solid which sublimes at room temperature.[19] X-ray diffraction was used to determine the dominant phase in the precursor after flash

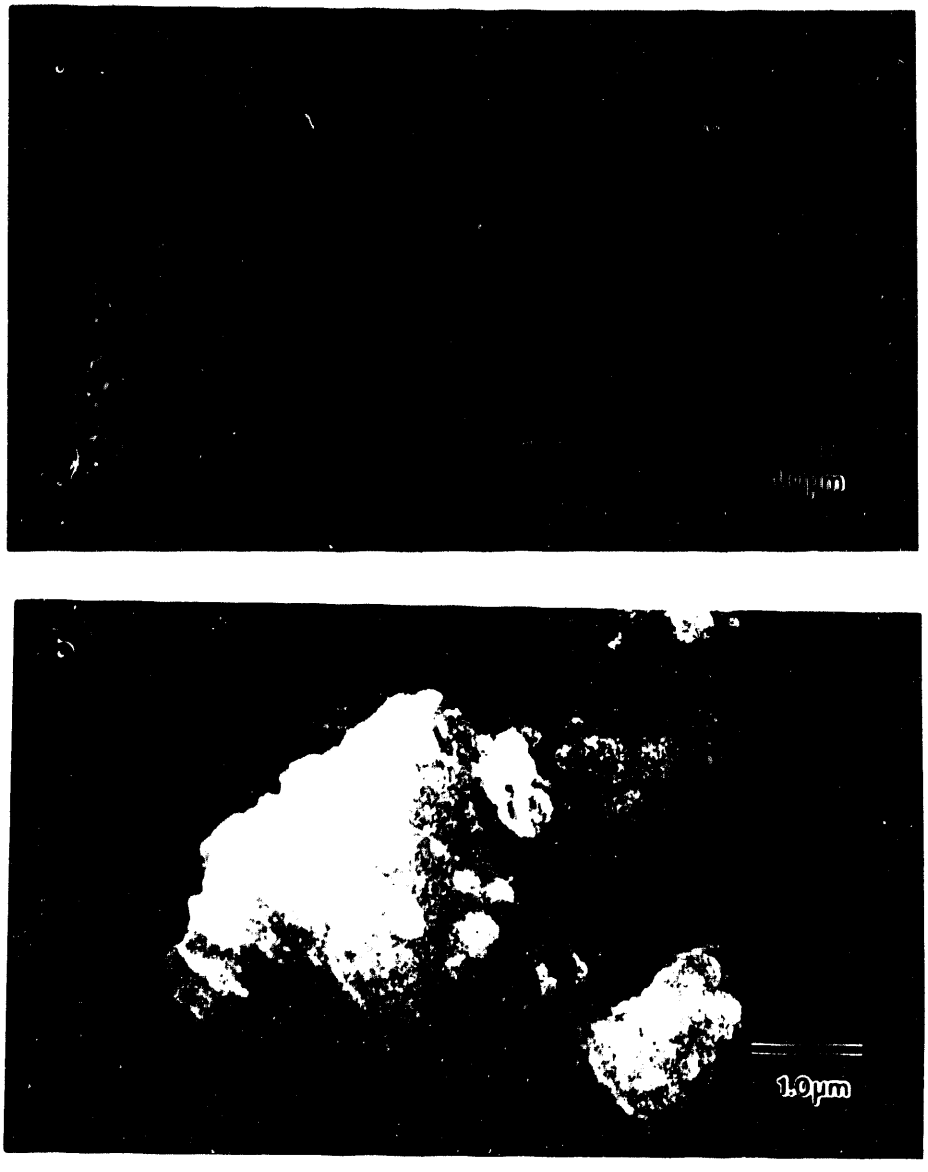

Figure 18. SEM secondary electron images, 15kV, 8mm WD
Gallium rich byproducts
a. overall view of sample b. close up of center of overall view

pyrolysis with the result being cubic GaP.[19] An SEM investigation was conducted on the GaP precursor after it had been pyrolized and is shown in Figure 18.

Characterization of the Nano-Compostites

Characterization was conducted on the composite powders with XRD, SEM and TEM methods used. The X-ray patterns for the as-prepared composite 006 (4 wt% GaP) and 007 (10.4 wt% GaP), shown in Figures 20 and 21, are almost identical to that of ZnS alone (Figure 19). The crystal structures of GaP and ZnS are identical and their lattice parameters only differ by 1.8% (Figure 1) which makes it very difficult to differentiate the compounds in a normal XRD pattern. A high resolution XRD scan was made of ZnS #56, composites 006, 007 and 008, all of which had been heat treated at 800°C for 20 hours. Figure 22 shows the high resolution XRD patterns of composite 008 (24 wt% GaP) and ZnS #56. Examination of this graph shows a shift in the large central peak (the [113] peak) to the left, probably caused by the GaP [113] peak at 55.9°. Inspection of the XRD of composite 008 (heat treated at 800°C for 20 hours), Figure 23, reveals a sizable shoulder developing on the [113] peak, further indication of the presence of GaP in its cubic form. The relatively low intensity of the X-ray signal from the GaP is suprising if one assumes the samples does indeed contain 24 wt% GaP. Subsequent analysis showed that this assumption was not valid.

Chemical analysis (by ICP methods) of some of the composite samples, shown in Table 4, shows that the composites did indeed contain gallium and phosphorus in significant amounts. However, the final amounts of gallium and phosphorus present in the samples is less than the original intended at the time of impregnation. This loss is partially due to the gallium and phosphorus being

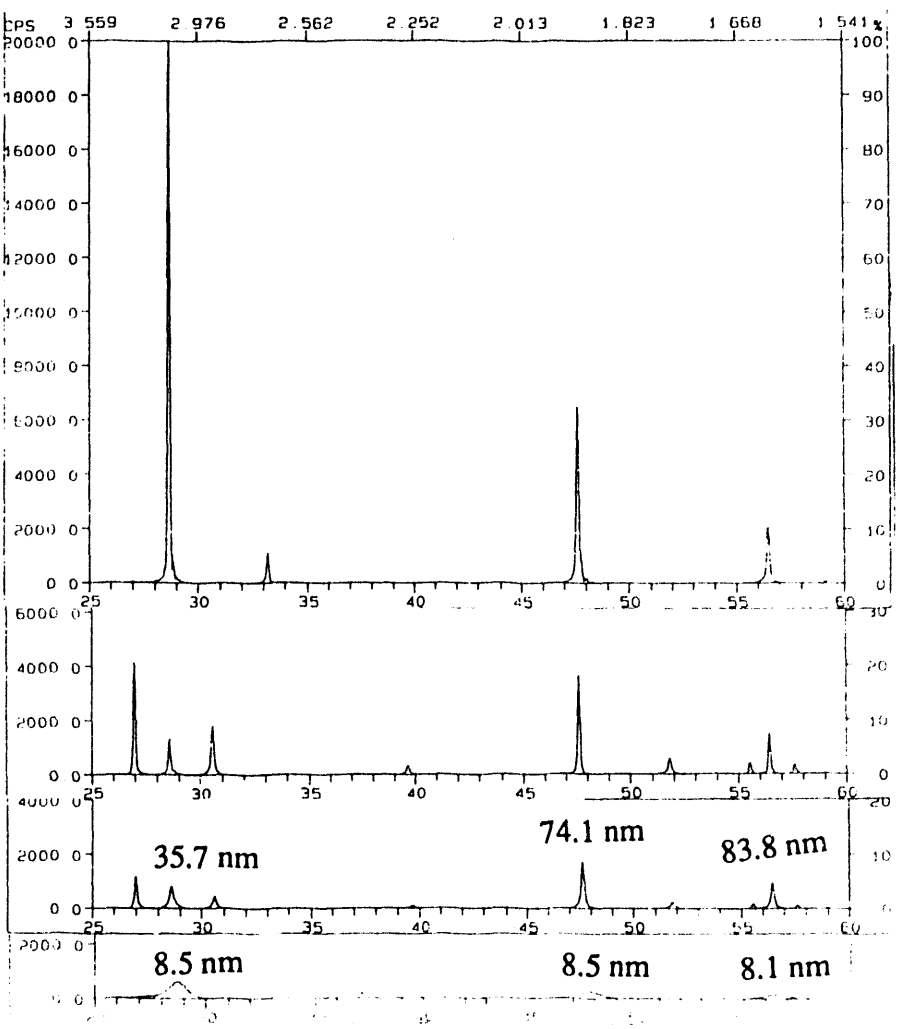

Figure 19. X-ray diffraction of ZnS #56 heat treated at several temperatures[10]
a) as-prepared b) 700°C for 20 hours
c) 800°C for 20 hours d) 900°C for 20 hours

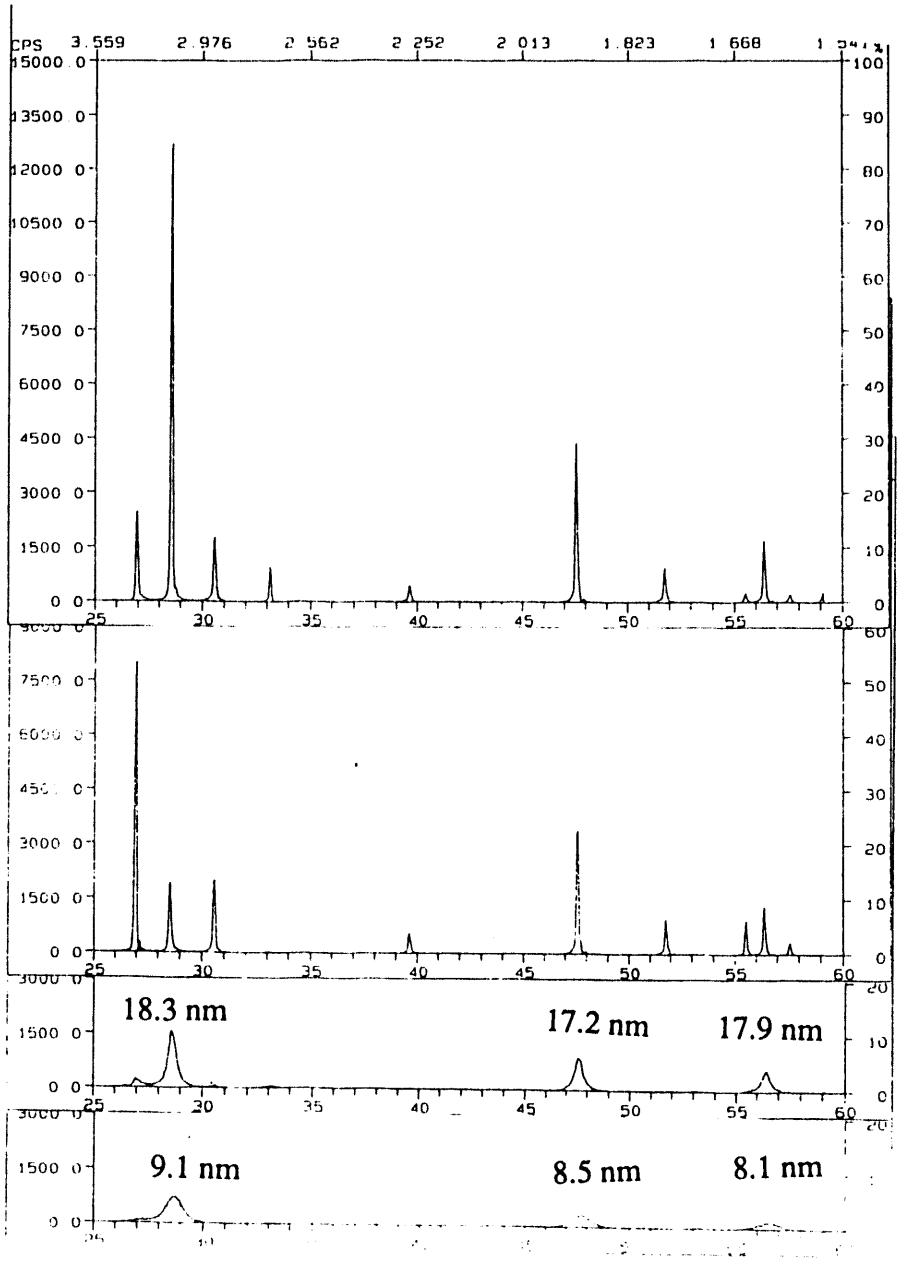

Figure 20. X-ray diffraction of composite 006 (4 wt% GaP) heat treated at several temperatures[10]
a) as-prepared b) 700°C for 20 hours
c) 800°C for 20 hours d) 900°C for 20 hours

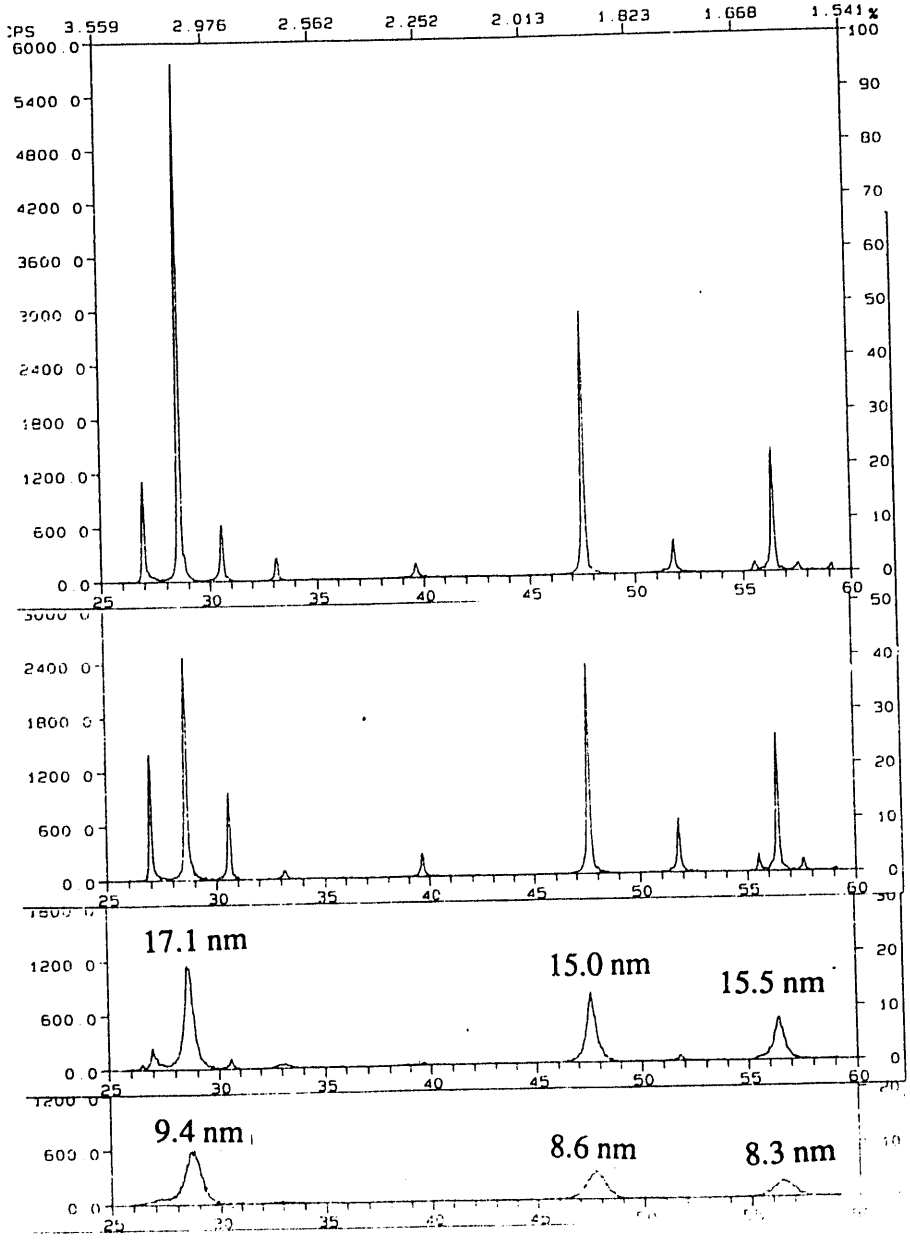

Figure 21. X-ray diffraction of composite 007 (10.4 wt% GaP) heat treated at several temperatures[10]
a) as-prepared b) 700°C for 20 hours
c) 800°C for 20 hours d) 900°C for 20 hours

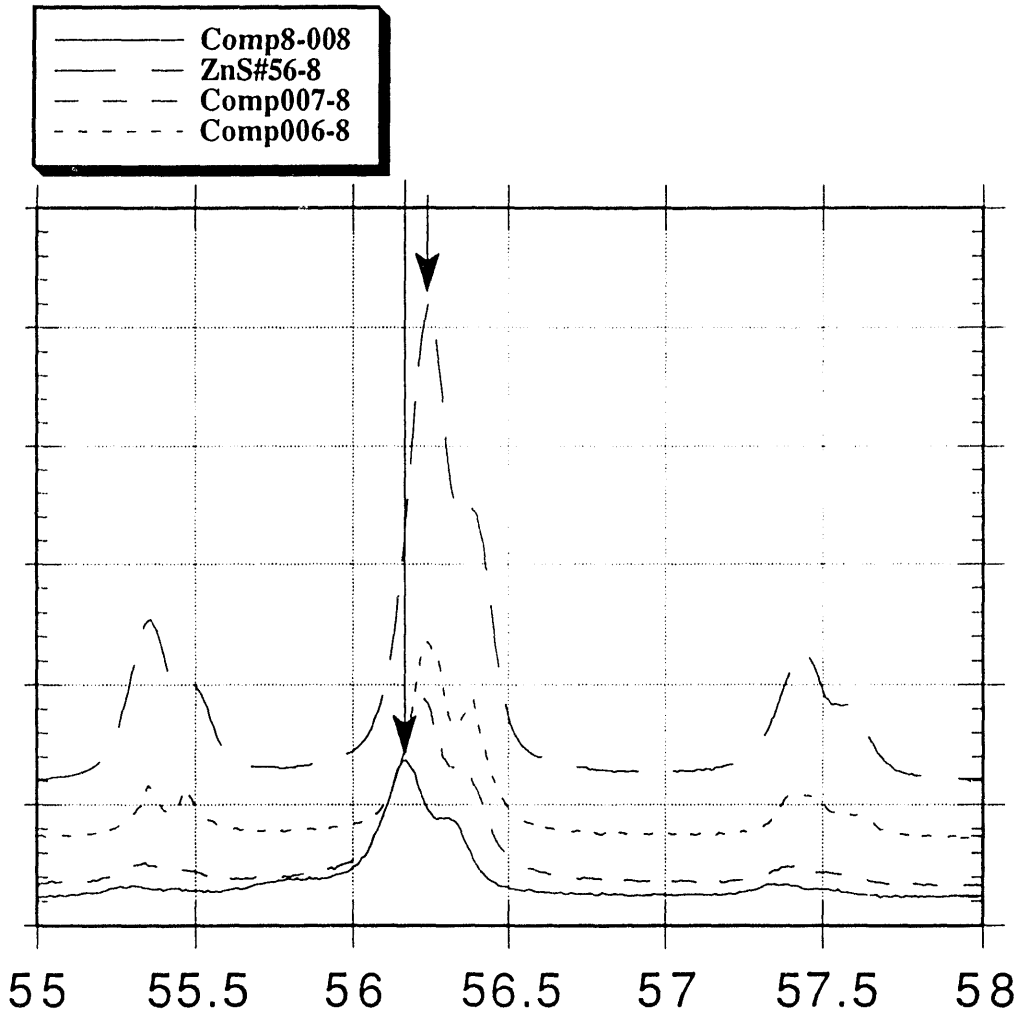

Figure 22. X-ray diffraction patterns for ZnS #56 and composite 008 (24 wt% GaP) heat treated at 800°C for 20 hours

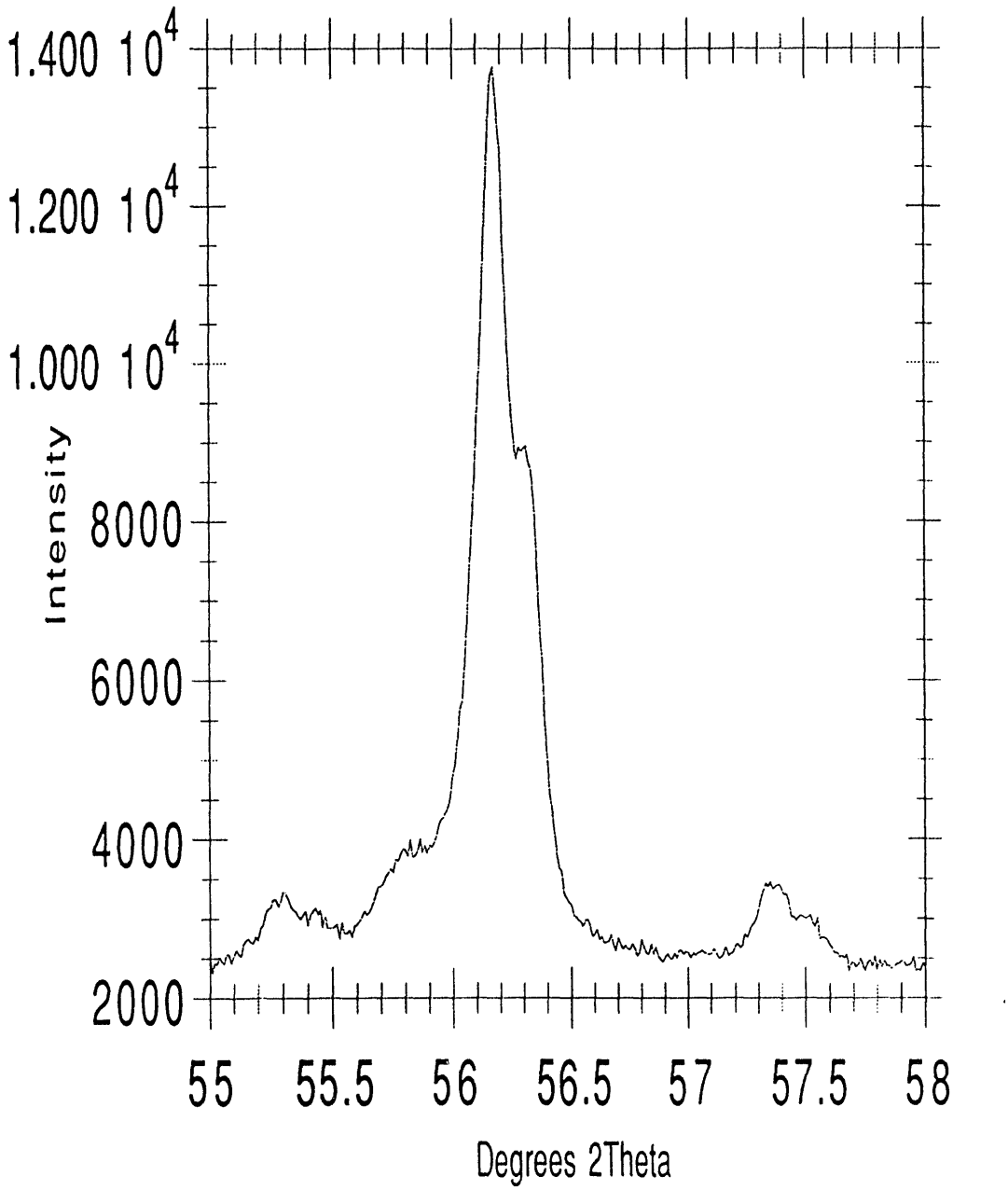

Figure 23. X-ray diffraction pattern for composite 008 (24 wt% GaP) heat treated at 800°C for 20 hours

Table 4. Chemical compositions of composite samples[10]

Sample	Heat Treatment	Target GaP wt %	Actual GaP wt %	Actual wt% Zn	S	Ga	P	S/Zn	P/Ga
ZnS #56	As-Prepared	0	0	67.63	31.55	0	0	0.95	0
ZnS #56	800°C for 20 hours	0	0	63.55	35.68	0	0	1.14	0
ZnS #56	900°C for 20 hours	0	0	62.76	35.38	0	0	1.15	0
Comp004	500°C for 20 hours	15.80	10.44	56.23	27.52	7.24	3.20	0.98	0.88
Comp006	As-Prepared	4.00	2.10	62.95	31.45	1.24	0.78	1.02	1.42
Comp006	800°C for 20 hours	4.00	1.30	63.89	31.12	0.70	0.55	0.99	1.77
Comp006	900°C for 20 hours	4.00	1.18	62.80	30.50	0.31	0.44	0.98	3.20
Comp007	As-Prepared	10.90	4.34	62.99	29.43	3.13	1.06	0.95	0.76
Comp007	800°C for 20 hours	10.90	1.88	65.45	31.37	1.21	0.65	0.98	1.21
Comp007	900°C for 20 hours	10.90	1.92	60.91	31.23	1.16	0.64	1.05	1.24
Comp008	As-Prepared	24							

deposited on the walls of the reaction chamber and partially due to vaporization of the compound. The small remaining amount of gallium and phosphorus in the samples explains the small peaks observed in the X-ray scans. The majority of the loss of gallium and phosphorus probably occurred in the initial reaction chamber where a yellow film formed and remained after the composite formation. Yellow is the natural color of the phosphino gallane compounds that were used to make the composites.[19]

SEM micrographs were also taken of the as-prepared nano-composites and are shown in Figure 24. These photos show that while the overall spherical microstructure of the powders is the same as that of ZnS the surface morphology is altered. In composite 004 (15.8 wt% GaP) the effect is most pronounced with the spheres looking smooth and having only a few nano-sized crystals on the surface, in contrast to the rough surface of the pure ZnS powders shown in Figure 6. This effect is caused by the GaP actually coating the outside of each sphere and filling in the spaces between each grain. The effect is not so pronounced in Figure 24b where the composite only has 10.4 wt% GaP.

The most revealing work done on the composite powders was that done using the TEM. Composites 004, 006, 007 and 008 were all examined with the TEM with results shown in Figures 29, 26a, 27a and 28a. These micrographs show that the nano-grained microstructure as well as the spherical overall microstructure is unaltered by the precursor material. It is only in composite 004 (15.8 wt% GaP) and 008 (24 wt% GaP) that the impregnated GaP precursor can be seen on the surfaces and in between some of the spheres (Figure 29 and 28 respectively). Energy Dispersive Spectroscopy (EDS) scans of 3 different particles in composite 004 (Figure 29), shown in Figures 30, 31 and 32, provide proof that the GaP precursor exists in

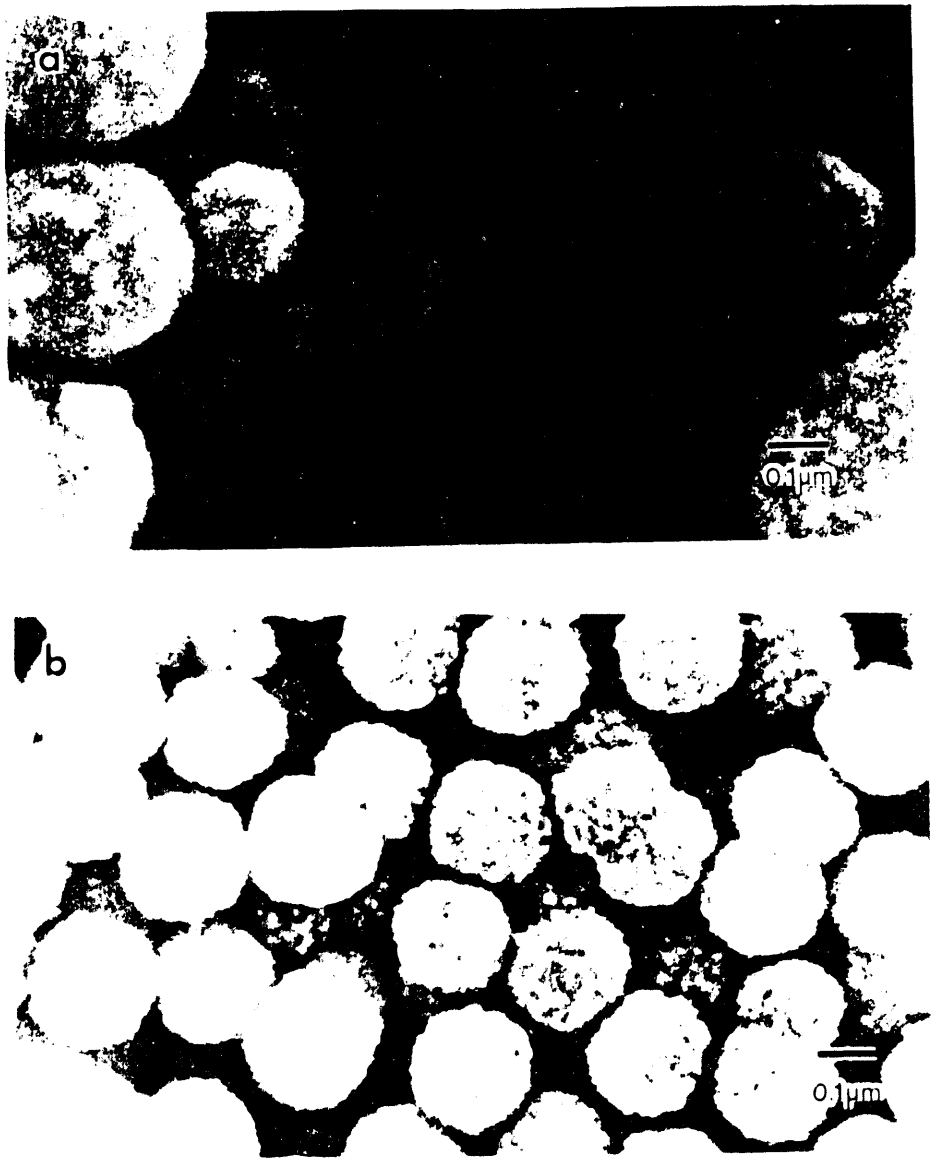

Figure 24. SEM secondary electron images, 15kV, 8 mm WD[10]
a) as-prepared composite 004 (15 wt% GaP)
b) as-prepared composite 007 (10.4 wt% GaP)

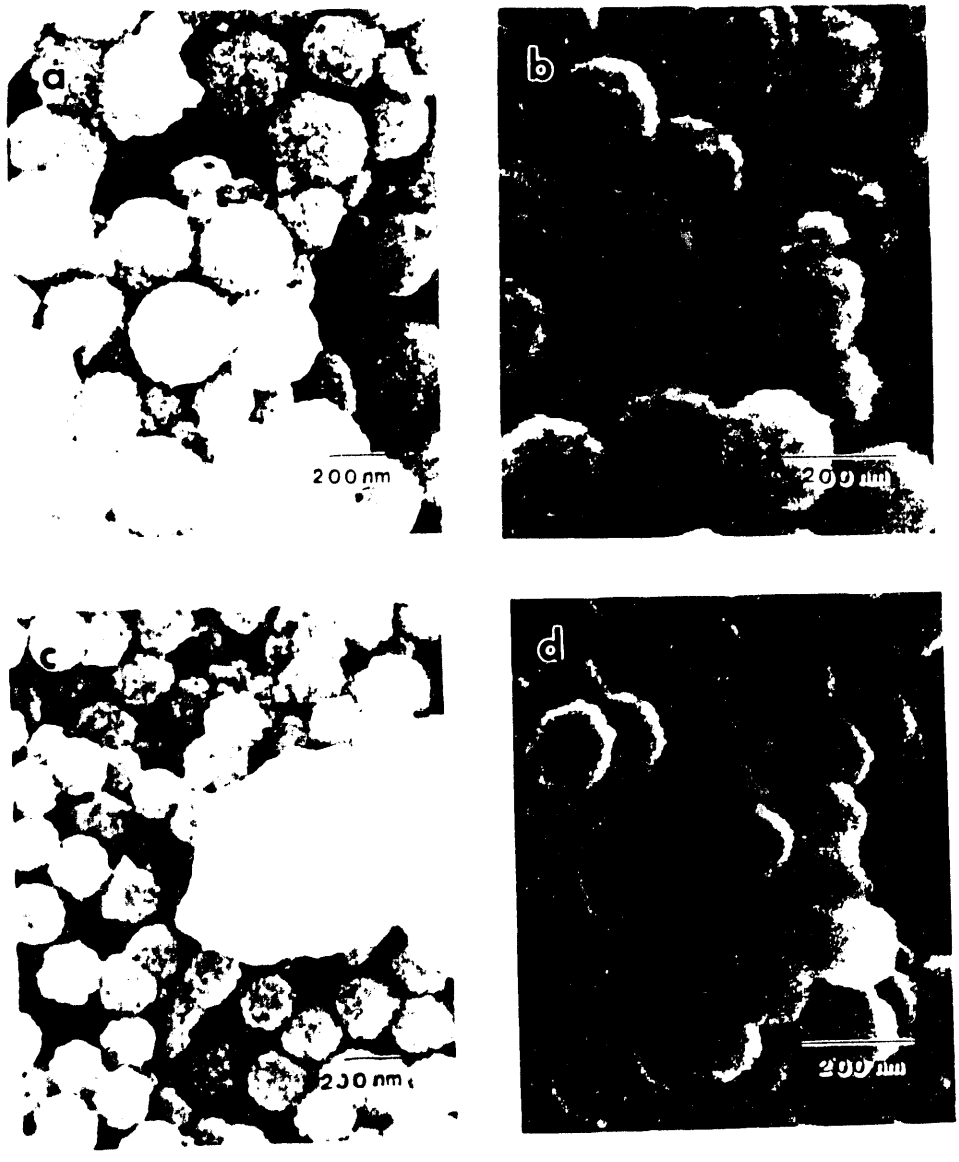

Figure 25. SEM secondary electron images, 15kV, 8 mm WD
composite 007 (10.4 wt% GaP) and 004 (15.8 wt% GaP) powders heat treated at several temperatures[10]
a) comp 004 500°C for 20 hours b) comp 007 700°C for 20 hours
c) comp 007 800°C for 20 hours d) comp 007 900°C for 20 hours

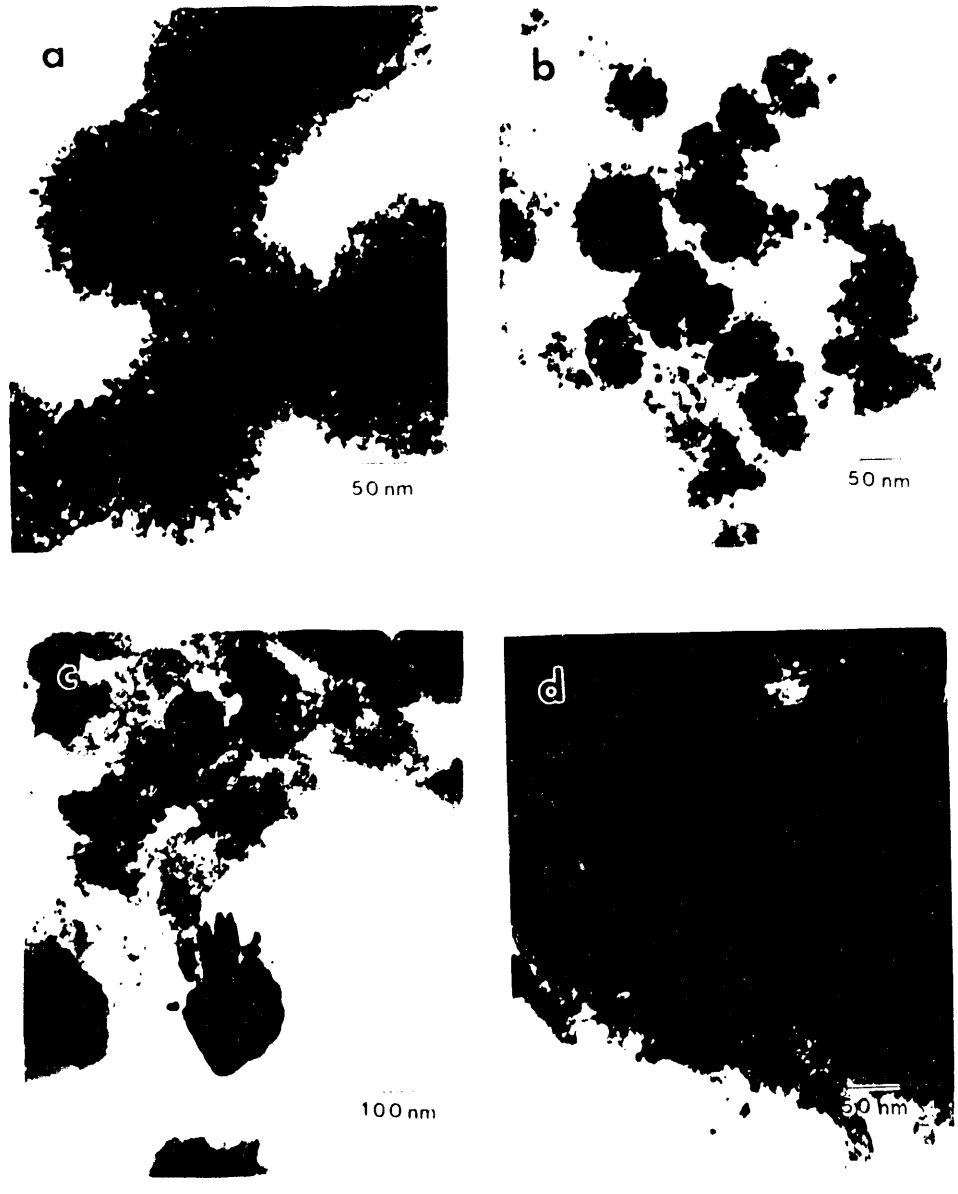

Figure 26. TEM bright field images, 300 kV
composite 006 (4 wt% GaP) heat treated at several temperatures
a) as-prepared b) 700°C for 20 hours
c) 800°C for 20 hours d) 900°C for 20 hours

Figure 27. TEM bright field images, 300 kV
composite 007 (10.4 wt% GaP) heat treated at several temperatures
a) as-prepared b) 700°C for 20 hours
c) 800°C for 20 hours

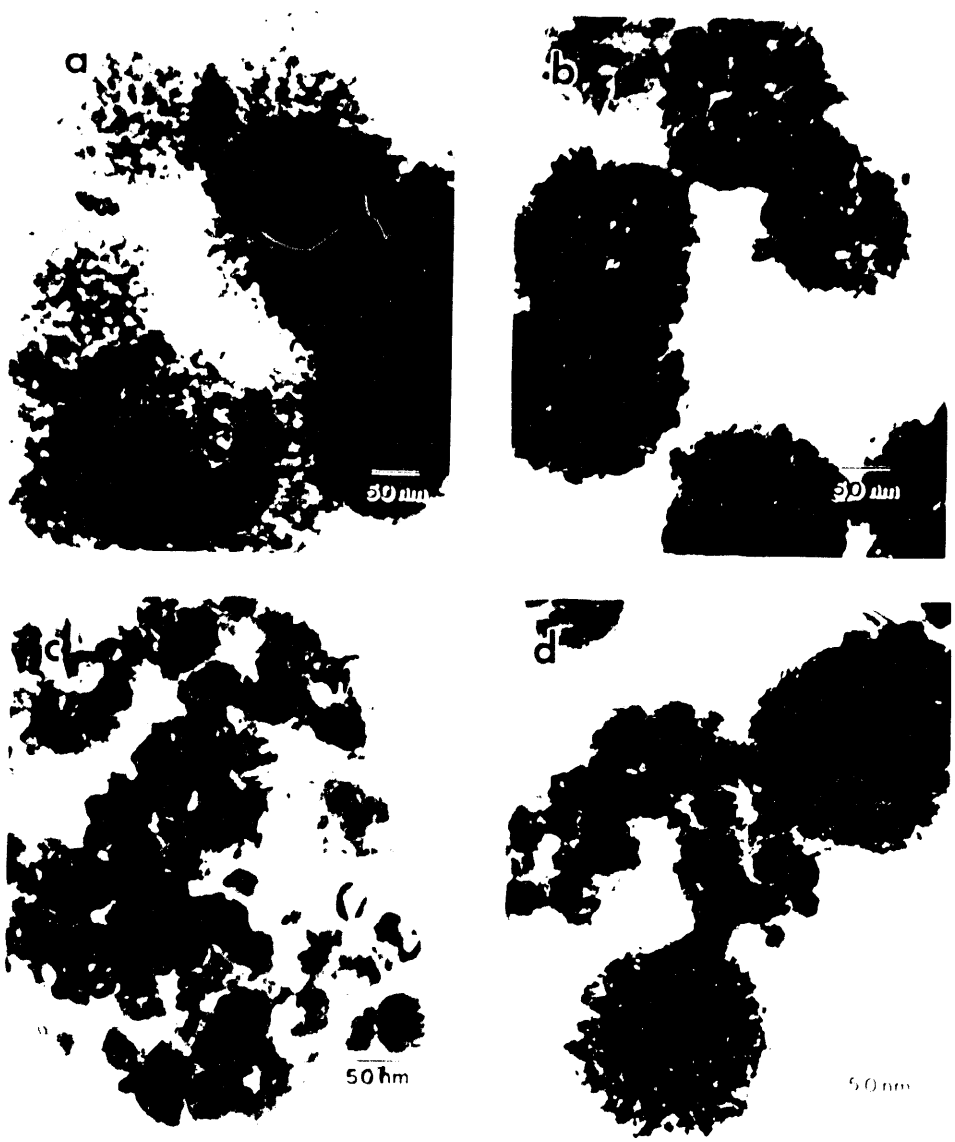

Figure 28. TEM bright field images, 300 kV
composite 008 (24 wt% GaP) heat treated at several temperatures
a) as-prepared b) 700°C for 20 hours
c) 800°C for 20 hours d) 900°C for 20 hours

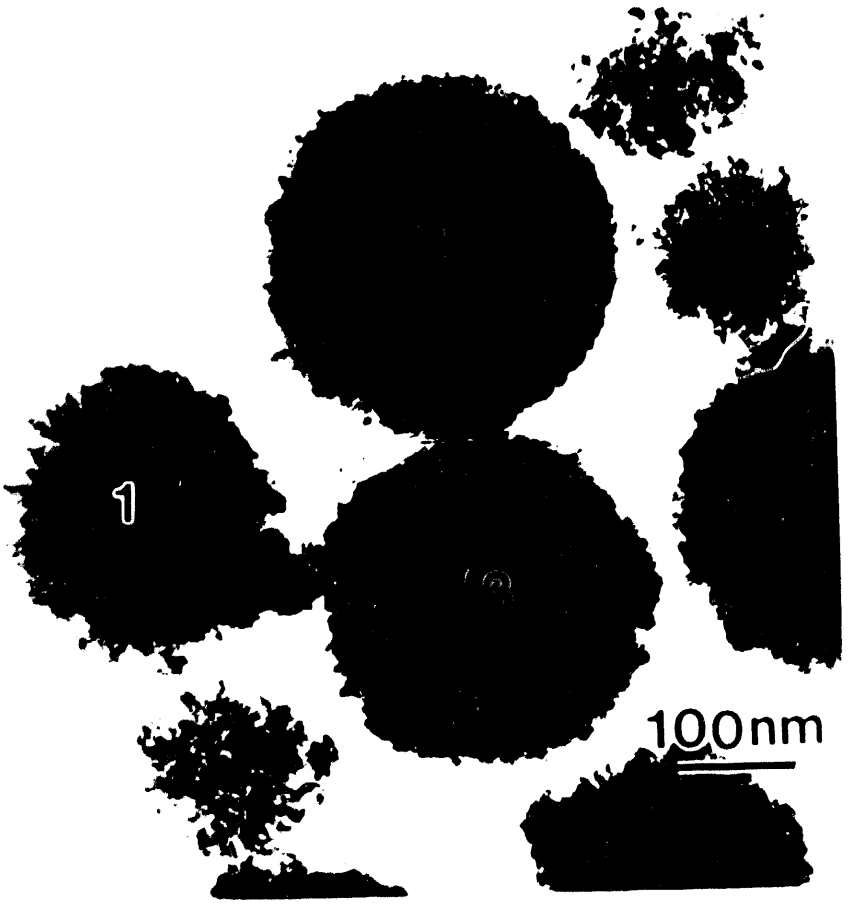

Figure 29. TEM bright field image, 300 kV
composite 004 (15.8 wt% GaP) as-prepared sample used for EDS

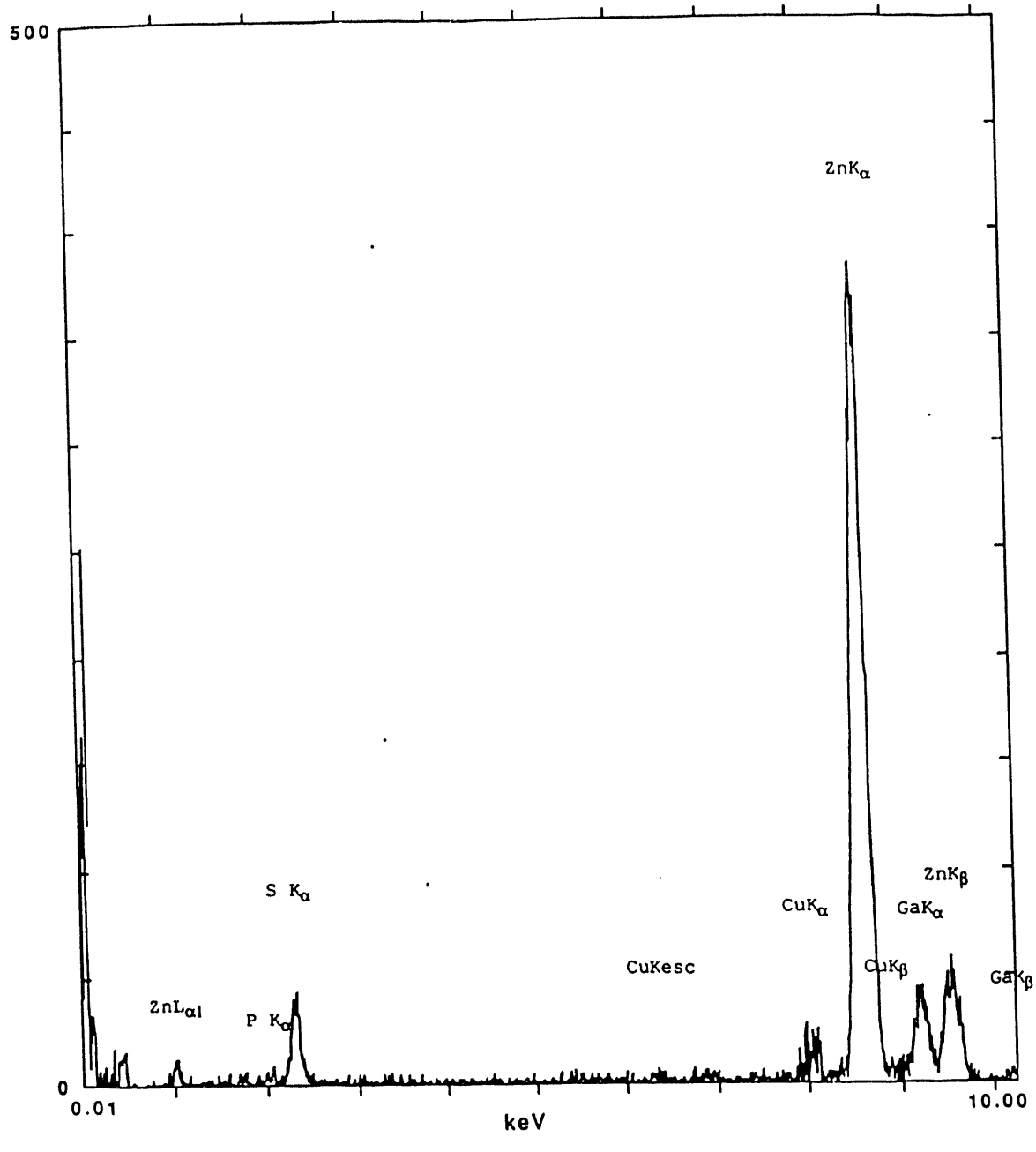

Figure 30. EDS scan for particle 1 on figure 29

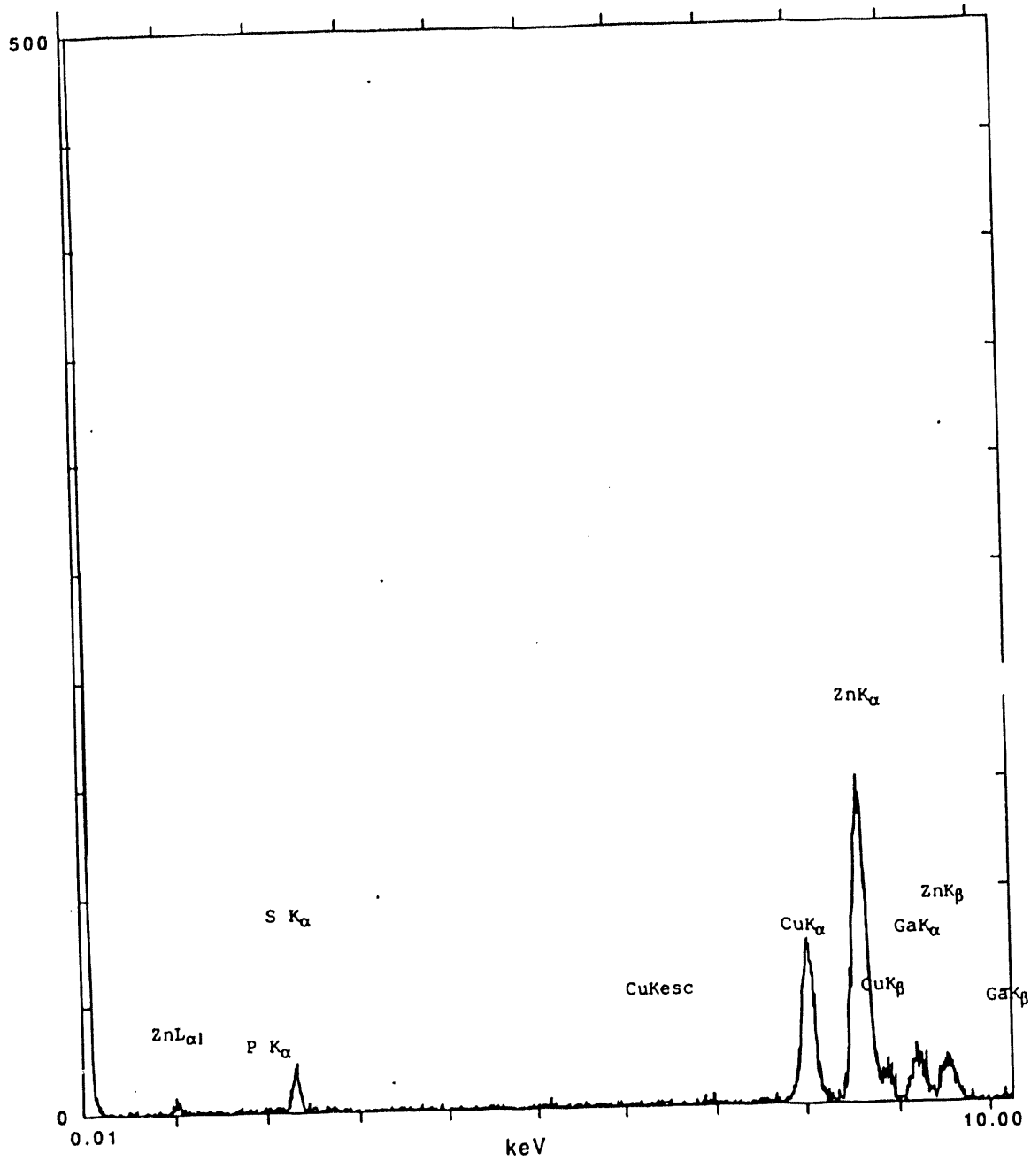

Figure 31. EDS scan for particle 2 on figure 29

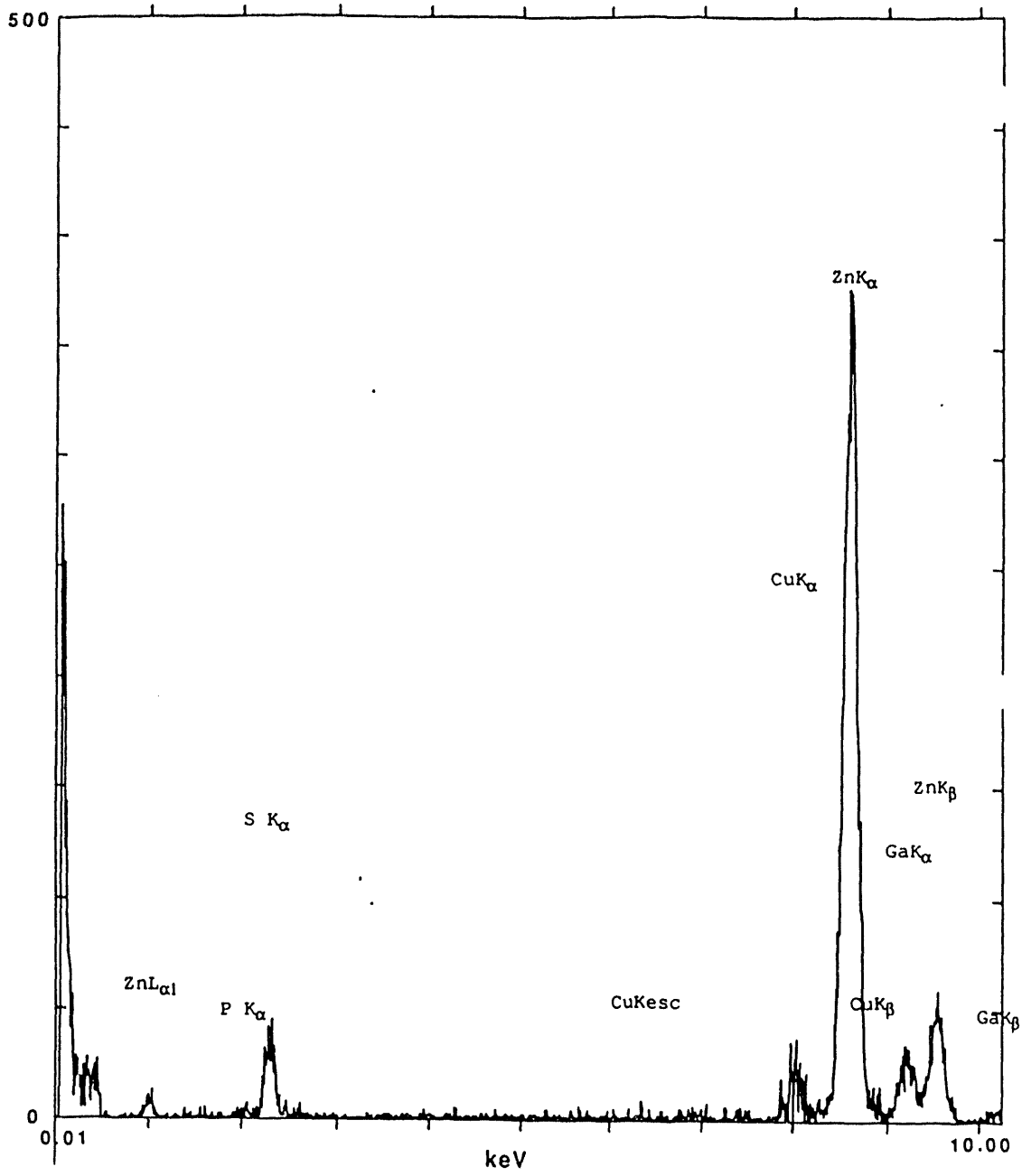

Figure 32. EDS scan for particle 3 on figure 29

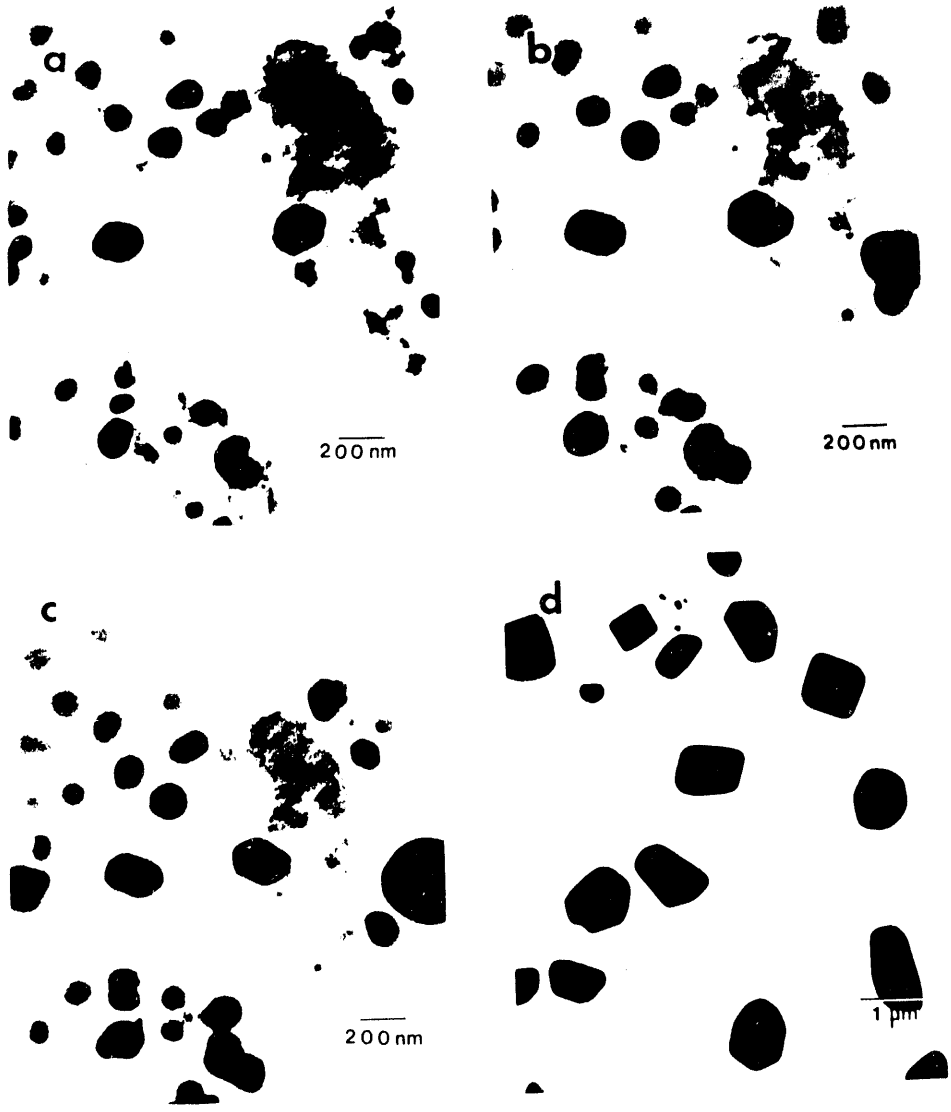

Figure 33. TEM bright field images, 300 kV
composite 007 (10.4 wt% GaP) in-situ heat treatment at 900°C
a) 900°C for 0 hours b) 900°C for 1 hour
c) 900°C for 2 hours d) 900°C for 4 hours

the spheres and has impregnated them to their centers. This claim can be made when one considers the very small area that the beam samples when condensed for EDS. When performing EDS the beam is focussed to a circle of approximately 10 nm diameter and centered in the area of the sample being examined. The electron beam only interacts with the material directly below the illuminated area, with minimal X-ray florescence from surrounding material. This small interaction volume minimizes the contribution to the X-ray signal (used in EDS) by other parts of the sample, consequently giving an accurate qualitative chemical composition of the specimen. Thus, the Ga and P detected is located either on the surface of the powder where the beam enters and exits the sphere, within the sphere itself, or a combination of the two possibilities. The relative strength of the signal indicates that a signifcant amount of Ga and P is present, more than what could be accounted for by a simple surface layer.

Heat Treatment of Composite Powders

Heat treatments of composite powders at temperatures ranging from 700 to 900°C were carried out to examine differences in the behavior of the powders upon heat treatment and to analyze the effects of different amounts of GaP precursor. These experiments yielded a large number of samples that were subsequently examined using XRD, SEM, TEM and chemical analysis. XRD was performed on composite 006 (4 wt% GaP) and composite 007 (10.4 wt% GaP) with the results shown in Figures 20 and 21; these results are contrasted with results from the identical heat treatments on pure ZnS shown in Figure 19. The ZnS shows significant grain growth (8.1 nm for as prepared to 64 nm for 700°C for 20 hours) and elimination of the hexagonal phase at 900°C. The composite samples show similar

initial grain size but retarded grain growth when compared to ZnS. The grain growth changes with respect to the composite examined, with composite 007 (10.4 wt% GaP) retarding more effectively than composite 006 (4 wt% GaP), due to the greater relative amounts of GaP. This lack of grain growth, which is confirmed in TEM (Figures 26-28) and SEM (Figure 25) investigations, suggests that the GaP is blocking the diffusion of ZnS, which in turn implies that the GaP must have impregnated the ZnS powders. Chemical analysis of the heat treated composite samples are shown in Table 4. Examination of these data show that the real amount of GaP in the sample is half of the target concentration. It is believed that most of the GaP loss occurs in the initial impregnation. Upon heating the relative amounts of zinc and sulfur are fairly constant but a consistent loss of both gallium and phosphorus is seen with the gallium loss exceeding that of phosphorus by a small margin. This loss may be due to the vaporization of free gallium, which has a low melting temperature.

SEM investigations of the heat treated composite powders as shown in Figure 25 show that while the overall microstructure is maintained, i.e. sub micron spheres, the fine nano-grained structure is obscured, presumably by GaP. The GaP precursor appears to coat the exterior of each sphere, filling the gaps between grains and giving the appearance of a smooth surface. Reaction of the precursor upon heat treatment results in a GaP shell on the surface of the powders. In the heat treated samples inconsistencies in the composites' behavior are observed, Figure 25c. This micrograph shows some powders that seem unaffected by the heat treatments, retaining both their general microstructure as well as their fine grains, while others have formed large agglomerates or even single crystals. This inconsistent behavior

suggests that the composite itself is inconsistent, due to non-uniform GaP impregnation.

The main thrust of the investigation was carried out using the TEM with as-prepared, heat treated and in-situ samples examined, Figures 26, 27, 28, 29, and 33. The fine microstructure of the as-prepared composite samples in Figures 26a, 27a, 28a and 29 are very similar to that of ZnS alone. Only with the use of the EDS was it possible to tell that anything was different, Figures 29-32. These chemical compositions were taken at various points on each particle, as indicated by each caption, and prove that there is gallium and phosphorus in both the interior and exterior of at least some of the particles. The TEM micrographs in Figures 26-28 show the composite powders structure as it relates to its respective heat treatment. The results correspond well to both the previous XRD and SEM results. Grain growth and the "hollowing" of each sphere can be seen in each set of micrographs just as in the pure ZnS samples. However, these phenomenae occurred in the ZnS samples at significantly lower temperatures (200°C difference). If one assumes the addition of GaP inhibits diffusion of ZnS, the slower growth kinetics of the composites seen in the interior of the spheres further indicates that the precursor material is able to infiltrate to the center of the spheres and fill the nano-sized pores present there. However, the micrograph in Figure 28d demonstrates inconsistencies of the composite forming process. All the particles in the group shown had been heat treated at 900°C for 20 hours and while some particles seem unaffected, retaining their nano-structures, significant grain growth is observed in others. Similar groups of particles were found in composite 006 and 007 but were not representative of the overall sample. It is believed that more careful impregnation of the powders will solve this problem.

During in-situ heat treatment experiments an interesting phenomenon was observed that was not seen in the heat treated samples, Figure 33. Large single crystals formed at various points on the carbon surface far removed from any groups of composite powders. These particles may have formed by vapor transport from the initial composite powders. Additional heating caused by the electron beam did not affect the formation of these particles since this phenomenon was observed at points in the sample that the beam had never touched. An effort to characterize these particles by way of electron diffraction only succeeded in melting the particles, due to the condensed beam causing heating.

SUMMARY AND CONCLUSIONS

ZnS Nanocrystalline Powders

Three different methods of ZnS production were examined. While the acetate method provided a reliable, consistent powder the considerable length of processing time and the inability of the powders to evenly absorb the GaP precursor make it the second choice for production of ZnS. The nitrate method produced powders that were more amenable to even impregnation of GaP, while the chloride method proved too erratic for any practical use.

The ZnS powders produced during this work displayed a mono-size, mono-dispersed, submicron, spherical, nanocrystalline-grained morphology which proved to be nano-porus. Sphalerite (cubic ZnS) is the dominant phase in both the as-prepared and heat treated samples. Grain growth is the dominant phenomenon observed at all temperatures with inter-particular growth (necking) occuring at temperatures above 700°C. A "hollowing" of the center of the spherical particles occurs at temperatures above 500°C; this phenomenon may be caused by differences between interior and exterior grain sizes. Upon heat treatment the larger exterior grains grow at the expense of the smaller interior grains, causing a hollow cavity to form. The grains themselves do not appear to be strongly bonded to each other. Evidence for this includes the smearing effect seen in polished samples and the numerous fractured particles seen in the fracture samples. This weak bonding is due to the large amount of porosity present in the spheres. This porosity allows the impregnation of precursor material into the spheres between the grains.

Sintering and grain growth occur even more readily in compacts of the nanocrystalline ZnS than in the loose powders, as expected. Full densification of

compacts of ZnS is not possible under normal heat treatments and so further measures such as hot pressing are required.

ZnS-GaP Nano-Composites

A. A. Naiini produced all the GaP precursors the results of which are available.[19]

It is apparent that the GaP precursor is impregnating the interiors of the individual ZnS powders and that subsequent flash pyrolysis converts the precursor into cubic GaP. Evidence for this includes the grain growth behavior of the microstructure upon heat treatment as compared to the grain growth characteristics of pure ZnS. GaP precursor is able to infiltrate the nano-pores of the ZnS particles and remain throughout heat treatments. The presence of GaP inhibits grain growth in the ZnS but apparently loss of gallium and phosphorus occurs during heat treatments causing the composites to have less GaP than expected. Impregnation of the ZnS powders with the precursor is very inconsistent on the macro scale. The method for infiltrating the precursor into the spheres needs to be improved so that more consistent, even impregnation of the ZnS particles occurs. Efforts to scale-up the production of composite powder are necessary to further this research since large amounts will be necessary to make IR window compacts.

Conclusions

Through extensive experimentation it has been possible to produce consistent, high quality nanocrystalline ZnS powders with grain sizes as small as 8 nm. These powders are nano-porous and are readily impregnated with GaP

precursor in a presently inconsistent manner. Both the crystal structure and small grain size of the ZnS can be maintained through the use of GaP. Heat treatment of the impregnated powders results in a ZnS - GaP composite structure where the grain sizes of the phases are on the order of 10-20 nm. Conventional powder processing techniques should be able to produce optically dense ceramic compacts with improved mechanical properties and suitable IR tranmission characteristics.

REFERENCES

1. Akinc, M.; Barton, T.; Chumbley, L. S.; Vedula, R., Research Proposal. Submitted to ONR, Proposal No. ERI-91075, September 12, 1990.
2. Dunn, B., Accelerated Research Initiative on 8-12 μm Transmitting Ceramics, Program Review, 19-20 September 1989, Silver Spring, MD.
3. Kloced, P.; Stone, L. E.; Boucher, M. W.; DeMilo, C., SPIE Int. Soc. Proc. Opt. Eng., 1988, 929, 65.
4. Gleiter, H., Encyclopedia of Physical Science and Technology, 1991 Yearbook; Academic Press, Inc., Amsterdam, p. 375 (1991).
5. Birringer, R.; Gleiter H., Advances in Material Science, Encyclopedia of Mat. Sci. and Eng. (edited by R.W. Cahn); Pergamon Press, Oxford, p. 339 (1988).
6. Goldstein, A. N.; Echer, C. M.; Alivisatos, A. P., "Melting in Semiconductor Nanocrystals," Science 256, 1425-1427, June 5 (1992)
7. Gleiter, H., Nanocrystalline Materials; Pergamon Press, Oxford, p. 297 (1990).
8. Sordelet, D. J.; Akinc, M., "Sintering of Monosized, Spherical Yttria Powders," J. Am. Ceram. Soc., 71(12), 1148-53 (1988).
9. Celikkaya, A.; Akinc, M., "Preparation and Mechanism of Formation of Spherical Submicron ZnS Powders," J. Am. Ceram. Soc. 73(8), 2360-65 (1990).
10. Han, Y., Department of MSE, Iowa State University, unpublished results.
11. Naiini, A.A. , Department of Chemistry, Iowa State University, unpublished results.
12. Richardson, K.; Akinc, M., "Preparation of Spherical Yttrium Oxide Powders Using Emulsion Evaporation," Ceramics International. 13, 253-61 (1987).

13. Willams, R.; Yocom, P. N.; Stofko, F. S., "Preparation and Properties of Spherical Zinc Sulfide Particles," Journal of Colloid and Interface Science, 106(2), 388-98 (1985).

14. Chiu, G., "The Preparation of Monodisperse Zinc Sulfide Sols," J. Colloid Interface Sci., 83 [1], 309-10 (1981).

15. Wilhelmy, D. M.; Matijevic, E., "Preparation and Properties of Monodispersed Spherical Collodial Particles of Zinc Sulfide," J. Chemical Soc., Faraday Trans. 1, 80, 563-70 (1984).

16. Celikkaya, A.; Akinc, M., "Morphology of Zinc Sulfide Particles Produced from Various Zinc Salts by Homogeneous Precipitation," J. Am. Ceramic Soc., 73 [2], 245-50 (1990).

17. Coates, G. E.; Grahm, J., "Trimethylgallium (III) Reaction with Diphenylphosphine and -Asine," J. Chem. Soc., 223, 1420-1423, (1963). and Beachley, O. T.; Coates, G.E., "Reactions of Trimethylaluminum, -Gallium, and Indinium with Some Primary and Secondary Phosphines and Arsines," J. Chem. Soc. , 3241, 2345-2349, (1965).

18. Cowley, A.H.; Benac, B. L.; Ekerdt, J.C.; Jones, R.A.; Kidd, K.B.; Lee, J.K.; Miller, J. E., "Chemical Vapor Deposition of III/V Compound Semiconductors with Novel Organometallic Precursors," J. Am. Chem. Soc., 110, 6248-6249, (1988).

19. Naiini, A. A.; Han, Y.; Akinc, M.; Verkade, J. G., "Synthesis and Thermolysis Studies of $(t\text{-Bu})_2GaPR_2$, R=i-Pr, t-Bu," being submitted to J. Am. Chem. Soc.

ACKNOWLEDGMENTS

I would like to thank the following people for their help and support during this research. Yong Han and Mufit Akinc for taking on a member in the middle of a project when mine got canceled. Fran Labbs for all his help in operating various equipment around the labs. Steve Martin for the use of his IR equipment. Lynn Gaskill and Krishna Vedula for helping me with my paperwork nightmare. All the faculty in the department for helping me at various times with various things.

Special thanks go Scott Chumbley, my major professor, for teaching me everything I know about electron microscopy and putting up with my weird schedule.

Special thanks also go to my parents whose love and support and encouragement helped me achieve my goals in education.

Lastly, extra thanks go to my loving future wife Jennifer Lusson who made me believe in myself and be proud of the things I could do.

This work was performed at Ames Laboratory, Iowa State University and was funded by a grant from the Office of Naval Research (1991)

APPENDIX

Instrumentation

X-ray diffraction

Phillips powder diffractometer PW1820 θ/2θ powder goinometer powered by a PW 1830 X-ray Generator
Operated at:
40 kV, 20 mA, step size of 0.05° 2θ and a two second integration time for each step.

Phillips Electronic Instruments Company
A division of North American Phillips Corporation
85 McKee Drive
Mahwah, New Jersey 07430

Siemens D500 diffractormeter

Siemens
Denver, Colorado

Electron Microscopes

Phillips CM30 Scanning/Transmission Electron Microscope (S/TEM)PW6040 operated at-
300 kV

Phillips Electronic Instruments Company
A division of North American Phillips Corporation
85 McKee Drive
Mahwah, New Jersey 07430

Hitachi Scanning Electron Microscope (SEM) operated at-
15 kV, 8 mm Working Distance (WD)

Energy Dispersive Spectrometer

Link Analytical Energy Dispersive Spectroscope (EDS) Model 5720

Oxford Instruments Incorporated
Analytical Systems Division
Oxford Instruments North America Incorporated

Microscope Products Division
Old Sauk Trails Park
8017 Excelsior Drive
Madison, Wisconsin 53717

TEM heated stage

Gatan Model 652 Double tilt heating holder

Gatan Incorporated
780 Commonwealth Drive
Warrendale (Pittsburgh), Pennsylvania 15086

Gold sputter coater

Technics Hummer sputter coater

Technics

Sonic disrupter

Tekmar sonic disrupter

Tekmar Company
Cincinnati, Ohio

DATE
FILMED
2/4/94
END